Geochemistry Geophysics Geosystems G3

Article
Volume 13, Number 10
19 October 2012
Q10014, doi:10.1029/2012GC004240
ISSN: 1525-2027

Published by AGU and the Geochemical Society

Cenozoic seawater Sr/Ca evolution

Sindia M. Sosdian
School of Earth and Ocean Sciences, Cardiff University, Cardiff CF10 3AT, UK (sosdians@cardiff.ac.uk)

Institute of Marine and Coastal Sciences and Department of Earth and Planetary Sciences, Rutgers, State University of New Jersey, New Brunswick, New Jersey 08901-8521, USA

Caroline H. Lear
School of Earth and Ocean Sciences, Cardiff University, Cardiff CF10 3AT, UK (learc@cardiff.ac.uk)

Kai Tao and Ethan L. Grossman
Department of Geology and Geophysics, Texas A&M University, College Station, Texas 77843-3115, USA (e-grossman@tamu.edu; taokai@gmail.com)

Aaron O'Dea
Smithsonian Tropical Research Institute, PO Box 0843-03092, Balboa, Panama (aaronodea@gmail.com)

Yair Rosenthal
Institute of Marine and Coastal Sciences and Department of Earth and Planetary Sciences, Rutgers, State University of New Jersey, New Brunswick, New Jersey 08901-8521, USA (rosentha@imcs.rutgers.edu)

[1] Records of seawater chemistry help constrain temporal variations in geochemical processes that impact the global carbon cycle and climate through Earth's history. Here we reconstruct Cenozoic seawater Sr/Ca (Sr/Ca_{sw}) using fossil *Conus* and turritellid gastropod Sr/Ca. Combined with an oxygen isotope paleotemperature record from the same samples, the gastropod record suggests that Sr/Ca_{sw} was slightly higher in the Eocene ($\sim$11.4 $\pm$ 3 mmol/mol) than today ($\sim$8.54 mmol/mol) and remained relatively stable from the mid- to late Cenozoic. We compare our gastropod Cenozoic Sr/Ca_{sw} record with a published turritellid gastropod Sr/Ca_{sw} record and other published biogenic (benthic foraminifera, fossil fish teeth) and inorganic precipitate (calcite veins) Sr/Ca_{sw} records. Once the uncertainties with our gastropod-derived Sr/Ca_{sw} are taken into account the Sr/Ca_{sw} record agrees reasonably well with biogenic Sr/Ca_{sw} records. Assuming a seawater [Ca] history derived from marine evaporite inclusions, all biogenic-based Sr/Ca_{sw} reconstructions imply decreasing seawater [Sr] through the Cenozoic, whereas the calcite vein Sr/Ca_{sw} reconstruction implies increasing [Sr] through the Cenozoic. We apply a simple geochemical model to examine the implications of divergence among these seawater [Sr] reconstructions and suggest that the interpretation and uncertainties associated with the gastropod and calcite vein proxies need to be revisited. Used in conjunction with records of carbonate depositional fluxes, our favored seawater Sr/Ca scenarios point to a significant increase in the proportion of aragonite versus calcite deposition in shelf sediments from the Middle Miocene, coincident with the proliferation of coral reefs. We propose that this occurred at least 10 million years after the seawater Mg/Ca threshold was passed, and was instead aided by declining levels of atmospheric carbon dioxide.

Components: 11,200 words, 9 figures, 1 table.

Keywords: gastropods; seawater chemistry; strontium.

Index Terms: 1050 Geochemistry: Marine geochemistry (4835, 4845, 4850); 1615 Global Change: Biogeochemical cycles, processes, and modeling (0412, 0414, 0793, 4805, 4912); 1635 Global Change: Oceans (1616, 3305, 4215, 4513).

Received 17 May 2012; **Revised** 29 August 2012; **Accepted** 18 September 2012; **Published** 19 October 2012.

Sosdian, S. M., C. H. Lear, K. Tao, E. L. Grossman, A. O'Dea, and Y. Rosenthal (2012), Cenozoic seawater Sr/Ca evolution, *Geochem. Geophys. Geosyst.*, *13*, Q10014, doi:10.1029/2012GC004240.

1. Introduction

[2] Reliable archives of ocean chemistry can be used to evaluate processes such as continental weathering, seafloor spreading, and carbonate deposition, and hence the coupling between geochemical cycles and global climate [*Broecker and Peng*, 1982; *Berner et al.*, 1983; *Delaney and Boyle*, 1986; *Wilkinson and Algeo*, 1989; *Ravizza and Zachos*, 2003]. Secular variations in seawater strontium concentration ([Sr]) are particularly interesting because they are thought to reflect long-term changes in continental weathering and carbonate deposition [*Turekian*, 1964]. The latter inference is a consequence of the fact that aragonite has a higher strontium distribution coefficient than calcite ($D_{Srarag} \approx 1$ versus $D_{Srcalc} \approx 0.1$) [*Kinsman and Holland*, 1969; *Katz et al.*, 1972] so shifts in the proportion of shelf aragonite deposition relative to deep-sea calcite deposition affect the seawater [Sr] concentration [*Graham et al.*, 1982; *Stoll and Schrag*, 2000].

[3] Documentation of changes in Cenozoic seawater Sr/Ca is limited as few methods exist for direct reconstruction of the elemental composition of seawater. Thus far records of past changes in Cenozoic seawater Sr/Ca (Sr/Ca_{sw}) derive from inorganic precipitates (e.g., marine barite and calcite veins), biogenic carbonate (e.g., foraminifera, corals, and molluscs), and biogenic apatite (e.g., fossil fish teeth enamel) [*Graham et al.*, 1982; *Steuber and Veizer*, 2002; *Averyt and Paytan*, 2003; *Lear et al.*, 2003; *Ivany et al.*, 2004; *Tripati et al.*, 2009; *Coggon et al.*, 2010; *Balter et al.*, 2011]. These studies yield conflicting Sr/Ca_{sw} records and leave the question of Sr/Ca_{sw} variations across the Cenozoic unresolved. Specifically, records from gastropods, benthic foraminifera, fish teeth, and ocean ridge calcium carbonate veins (CCVs) indicate that Sr/Ca_{sw} was respectively ~50% higher, ~15 and 20% lower, or ~70% lower at 40 Ma than today [*Lear et al.*, 2003; *Tripati et al.*, 2009; *Coggon et al.*, 2010; *Balter et al.*, 2011], suggesting that the geochemical systematics and/or underlying assumptions for these proxy reconstructions are poorly understood. For example, it is possible that benthic foraminiferal Sr/Ca is also affected by carbonate saturation state [*Dissard et al.*, 2010; *Raitzsch et al.*, 2010]. The interpretation of Sr/Ca_{sw} reconstructions derived from fossil fish teeth may be complicated by changes in the diet of the sharks and rays [*Balter and Lécuyer*, 2010]. The ocean ridge CCV method uses extrapolation to determine seawater chemistry from evolved hydrothermal fluids. This requires accurate calculation of the age and temperature of the fluids and a full understanding of the CCV partition coefficients [*Coggon et al.*, 2010]. Although the seawater Mg/Ca records obtained using this method agree with some other proxies, the markedly different results for Sr/Ca_{sw} remain a conundrum [*Coggon et al.*, 2010; *Broecker and Yu*, 2011; *Coggon et al.*, 2011].

[4] Several studies have shown that mollusc shell Sr/Ca is controlled by ambient solution and could provide a record of Sr/Ca_{sw} [*Buchardt and Fritz*, 1978; *Lorens and Bender*, 1980]. Temperature and growth rate also modify Sr/Ca in modern and fossil marine gastropods [*Purton et al.*, 1999; *Sosdian et al.*, 2006; *Gentry et al.*, 2008; *Tripati et al.*, 2009]. These relationships have been used in a study of turritellid gastropods to suggest that between 64 and 37 Ma, Sr/Ca_{sw} was higher than today [*Tripati et al.*, 2009], in contrast with results based on other biogenic and abiogenic proxies [*Lear et al.*, 2003; *Coggon et al.*, 2010; *Balter et al.*, 2011]. However, this gastropod record did not always use paired Sr/Ca-$\delta^{18}O$ data from the same shell to correct for temperature (i.e., the Sr/Ca ratios of 13 out of 15 fossil shells were temperature corrected using external Mg/Ca and $\delta^{18}O$ estimates based on different proxies). Here we reassess the gastropod Sr/Ca_{sw} proxy with new seasonally resolved, paired $\delta^{18}O$-Sr/Ca analyses of 34 fossil *Conus* and turritellid gastropod shells. We produce a new Sr/Ca_{sw} record spanning the last 42 Ma and critically evaluate differences between this and other published records.

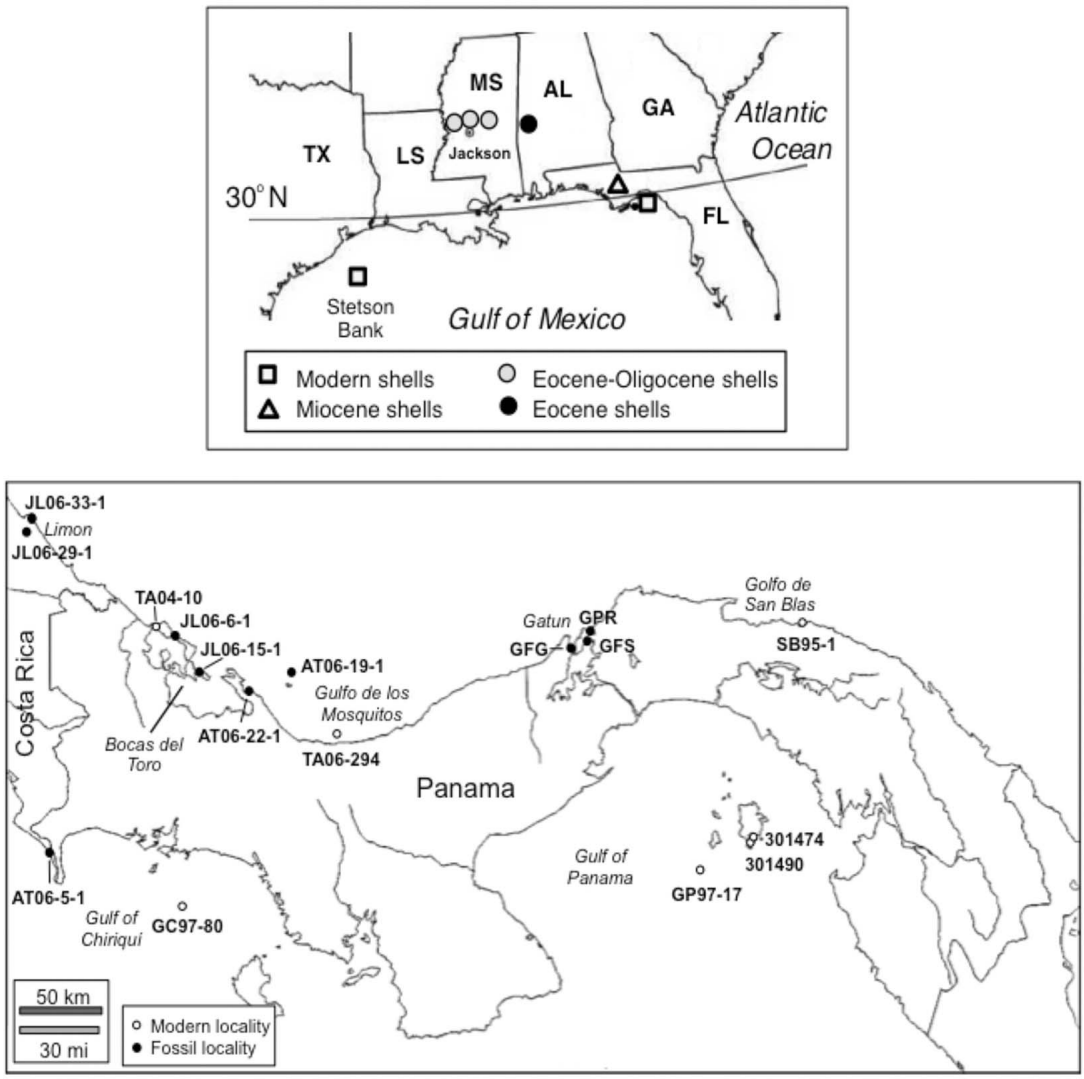

Figure 1. (top) Localities of samples collected in Mississippi, Alabama, and Florida. Localities for Mississippi, Alabama, and Florida Panhandle are denoted by the first two letters of the sample identification number, which represents the formation or member name (e.g., CF = Chipola formation as in CFC-1). (bottom) Localities of samples collected from Panama and Costa Rica.

[5] Combining records of seawater chemistry with geochemical models provides a platform to evaluate long-term controls on the cycling of major ions in the ocean across multiple time scales (i.e., kyr to Myr) [e.g., *Graham et al.*, 1982; *Hardie*, 1996; *Stoll and Schrag*, 1998; *Steuber and Veizer*, 2002; *Arvidson et al.*, 2006]. Geochemical modeling studies of Sr/Ca_{sw} hypothesize that large shifts in Sr/Ca_{sw} ratios from the Phanerozoic to Cenozoic resulted from changes in riverine input, mid-ocean ridge spreading rate, diagenetic recycling flux and the proportion of aragonite versus calcite deposition [*Graham et al.*, 1982; *Schlanger*, 1988; *Steuber and Veizer*, 2002]. We use a simple mass balance model to examine the implications of the contradictory seawater Sr/Ca reconstructions and speculate on the links between the global carbon and strontium cycles via Cenozoic coral reef development.

2. Methods

2.1. Study Area and Samples

[6] Fossil gastropods were collected from 20 localities on the U.S. Gulf Coast, Panama, and Costa Rica (Figures 1 and 2). Twenty-eight *Conus* and six turretillid shells were collected from 17 formations spanning the Eocene to Pleistocene (Table 1) [*Kobashi et al.*, 2001; *Tao and Grossman*, 2010; *Tao*, 2012]. Seventeen Modern *Conus* specimens of

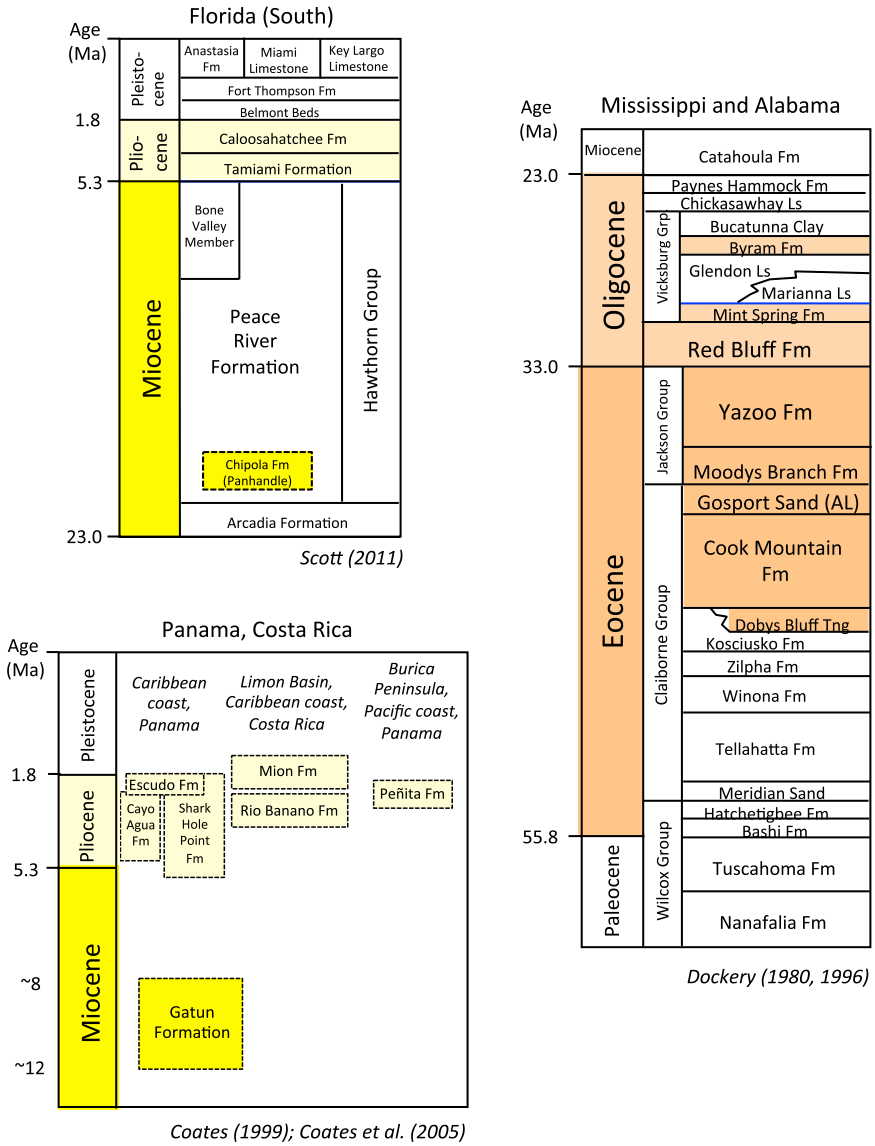

Figure 2. Stratigraphy of South Florida, Mississippi, Alabama, Panama and Costa Rica. Highlighted epochs and stratigraphic units are those for which there are gastropod Sr/Ca data [*Dockery*, 1980, 1996; *Coates*, 1999; *Coates et al.*, 2005; *Scott*, 2011].

11 different species were collected from the U.S. Gulf Coast, the Caribbean and the Pacific Ocean [*Kobashi et al.*, 2001; K. Tao et al., Quantifying upwelling and freshening in nearshore tropical environments using stable isotopes in modern Tropical American mollusks, submitted to *Bulletin of Marine Science*, 2012] (Table 1). Age estimates and the associated uncertainties for the fossil shells collected in this study from the U.S. Gulf Coast, Panama, and Costa Rice are listed in Table 1. Foraminiferal oxygen isotope ($\delta^{18}O$) analyses suggest that the Pleistocene specimens collected from the Moin Formation in Costa Rica were derived from glacial horizons (L. Collins, personal communication, 2011). Unfortunately, Milankovitch-scale stratigraphic information is not available for the remaining fossil samples.

[7] We estimated seawater temperature from the $\delta^{18}O$ of the same shell using the *Grossman and Ku* [1986] aragonite paleotemperature equation. Oxygen isotope analyses were performed at Texas A&M University (TAMU) using a Finnigan MAT 251 isotope ratio mass spectrometer (IRMS) and Kiel II automated carbonate reaction system for modern and fossil U.S. Gulf Coast mollusks [*Kobashi et al.*, 2001; *Gentry et al.*, 2008], a Thermo-Finnigan DeltaXP IRMS and GasBench II automated gas-handling system for Neogene and modern mollusks from Florida and Panama

Table 1. Locality Information, Sr/Ca and $\delta^{18}O$ Data of Mollusks, and Calculated Temperature Sensitivities (mmol mol^{-1} per °C) Derived From Seasonal Sr/Ca and $\delta^{18}O$ Profiles[a]

Sample ID	Modern Specimen Locality or Fossil Specimen Geologic Unit	Species	Avg. Age (Ma)	Age Uncertainty (Ma)	$\delta^{18}O$-Sr/Ca Correlation, R^2	Sr/Ca (mmol mol^{-1})			$\delta^{18}O$ (‰)		Calc. Temp. Sensitivity (mmol mol^{-1} $°C^{-1}$)	Data Sources[h]	
						Mean	Max.	Min.	Max.	Min.		$\delta^{18}O$	Sr/Ca
FGS1, FGS3, FGS4	Stetson Bank, GOM	*Conus ermineus*	0	-	0.64	1.5	1.8	1.1	1.3	−1.3	0.09	G08	S06
TA06-294A	Golfo de los Mosquitos, PN	*Conus spp.*	0	-	0.11	2.1	2.4	1.9	−0.5	−1.3	0.14	T13	TUD
SB95-1	San Blas, PN	*Conus mus*	0	-	0.27	1.6	2.2	1.4	−0.9	−2.5	0.12	T13	TUD
TA04-10A	Bocas del Toro, PN	*Conus jaspideus*	0	-	0.24	2.1	3.0	1.8	−0.5	−1.4	0.30	T13	TUD
TA04-10B	Bocas del Toro, PN	*Conus jaspideus*	0	-	0.37	1.9	2.5	1.6	−0.5	−1.2	0.27	T13	TUD
GP97-17A	Golfo de Panama, PN	*Conus recurvus*	0	-	0.13	1.9	2.3	1.4	−0.3	−3.5	0.06	T13	TUD
GP97-17B	Golfo de Panama, PN	*Conus mahogani*	0	-	0.11	2.0	2.9	1.5	−1.1	−3.4	0.14	T13	TUD
GC97-80A	Golfo de Chirquí, PN	*Conus arcuatus*	0	-	0.003	2.1	2.7	1.6	0.8	−0.5	0.18	T13	TUD
GC97-80B	Golfo de Chirquí, PN	*Conus arcuatus*	0	-	0.8	1.5	1.6	1.4	1.1	−0.2	0.04	T13	TUD
301474	Golfo de Panama, PN	*Conus patricius*	0	-	0.43	1.9	2.4	1.5	−0.5	−3.4	0.07	T13	TUD
301490A	Golfo de Panama, PN	*Conus ximenes*	0	-	0.35	2.3	3.4	1.7	0.2	−2.5	0.15	T13	TUD
301490B	Golfo de Panama, PN	*Conus ximenes*	0	-	0.57	2.2	2.4	1.8	−0.5	−2.9	0.06	T13	TUD
MOC1	Stetson Bank, GOM	*Conus ermineus*	0	-	0.14	1.1	1.4	0.9	1.2	−0.4	0.08	K01	S13
MOC3	Alligator Point, GOM	*Conus floridanus*	0	-	0.15	1.8	2.2	1.3	1.7	−1.3	0.07	K01	S13
MOC8	Stetson Bank, GOM	*Conus spp.*	0	-	0.15	1.5	1.9	1.2	1.3	−0.9	0.08	GUD	S13
JL06-33-1C	Mion fm, CR	*Conus spp.*	1.6[b]	1.5–1.7	0.43	2.42	2.5	2.2	0.5	−0.4	0.09	T12	TUD
JL06-33-1F	Mion fm, CR	*Conus spp.*	1.6[b]	1.5–1.7	0.47	2.55	2.8	2.1	0.6	−0.5	0.14	T12	TUD
AT06-29-1A	Rio Banano fm, CR	*Conus spp.*	3.05[b]	2.9–3.2	0.04	2.31	3.2	1.4	−0.1	−1.4	0.34	T12	TUD
AT06-29-1B	Rio Banano fm, CR	*Conus spp.*	3.05[b]	2.9–3.2	0.28	2.61	2.9	2.1	−0.5	−2.2	0.10	T12	TUD
PTF-1B1	Pinecrest Beds, FL	*Turritella gladeensis*	3.25[c]	3.0–3.5	0.13	2.3	2.5	2.1	1.0	−1.2	0.04	T10	T10
PTF-1B2	Pinecrest Beds, FL	*Turritella gladeensis*	3.25[c]	3.0–3.5	0.002	2.4	2.6	2.2	2.0	−0.7	0.03	T10	T10
PTF-3A	Pinecrest Beds, FL	*Conus spurius*	3.25[c]	3.0–3.5	0.40	1.9	2.3	1.5	0.8	−0.8	0.12	T10	T10
61689	Pinecrest Beds, FL	*Conus adversarius*	3.25[c]	3.0–3.5	0.45	2.0	2.3	1.6	1.1	−0.9	0.08	T10	T10
AT06-5-1A	Peñita fm, CR	*Conus spp.*	3.55[d]	3.5–3.6	0.35	2.40	3.0	1.9	0.1	−1.9	0.12	T12	TUD
AT06-5-1B	Peñita fm, CR	*Conus spp.*	3.55[d]	3.5–3.6	0.41	2.10	2.5	1.8	0.2	−1.3	0.10	T12	TUD
AT06-19-1	Escudo de Veraguas fm, PN	*Conus spp.*	3.55[b]	3.5–3.6	0.35	2.47	2.7	2.0	1.4	0.0	0.12	T12	TUD
JL06-15-1	Cayo Agua fm, PN	*Conus spp.*	4.25[b]	3.5–5.0	0.11	3.61	4.4	2.7	−0.2	−1.3	0.36	T12	TUD
AT06-22-1A	Shark Hole Point fm, PN	*Conus spp.*	5.65[b]	5.6–5.7	0.02	2.30	3.2	1.9	0.3	−0.2	0.60	T12	TUD
GFG-A	Gatun fm, PN	*Conus spp.*	8[b]	±0.5[g]	0.26	2.60	3.0	2.0	0.1	−1.2	0.19	T12	TUD
GPR-A	Gatun fm, PN	*Conus spp.*	11.5[b]	11.0–12.0	0.47	2.48	3.0	2.0	−0.6	−1.7	0.20	T12	TUD
GFS-3A	Gatun fm, PN	*Conus spp.*	11.5[b]	11.0–12.0	0.42	2.60	3.0	1.9	−0.2	−2.0	0.14	T12	TUD
GFS-3B	Gatun fm, PN	*Conus spp.*	11.5[b]	11.0–12.0	0.26	2.69	3.1	2.3	−0.8	−1.7	0.19	T12	TUD
GFS-3F	Gatun fm, PN	*Conus spp.*	11.5[b]	11.0–12.0	0.65	2.53	2.9	2.1	−0.7	−1.9	0.17	T12	TUD
CFC-1	Chipola fm., FL	*Conus sulculus*	18.6[e]	±1.0[g]	0.45	2.3	3.0	1.7	0.2	−2.0	0.13	K01	S13
BFC-1	Byram fm., MS	*Conus alveatus*	30[f]	±1.0[g]	0.67	2.6	3.2	2.2	1.6	−1.3	0.08	K01	S13
BFC-3	Byram fm., MS	*Conus alveatus*	30[f]	±1.0[g]	0.25	2.6	3.5	2.0	1.1	−1.2	0.16	K01	S13

Table 1. (continued)

Sample ID	Modern Specimen Locality or Fossil Specimen Geologic Unit	Species	Avg. Age (Ma)	Age Uncertainty (Ma)	δ^{18}O-Sr/Ca Correlation, R^2	Sr/Ca (mmol mol^{-1})			δ^{18}O (‰)		Calc. Temp. Sensitivity (mmol mol^{-1} °C^{-1})	Data Sources[h]	
						Mean	Max.	Min.	Max.	Min.		δ^{18}O	Sr/Ca
MSC-1	Mint Spring fm., MS	*Conus alveatus*	32[f]	±1.0[g]	0.44	2.1	2.5	1.8	1.1	−0.7	0.09	K01	S13
MSC-2	Mint Spring fm., MS	*Conus alveatus*	32[f]	±1.0[g]	0.94	2.3	3.4	1.8	0.7	−0.7	0.27	K01	S13
RBC-1	Red Bluff fm., MS	*Conus alveatus*	33[f]	±1.0[g]	0.90	2.5	3.3	1.8	1.2	−0.2	0.26	K01	S13
RBC-3	Red Bluff fm., MS	*Conus alveatus*	33[f]	±1.0[g]	0.28	2.5	3.3	2.1	1.4	−0.2	0.19	K01	S13
YCC-1	Yazoo fm., MS	*Conus spp*	36[f]	±1.0[g]	0.25	2.2	3.3	1.7	0.2	−0.4	0.65	K01	S13
MBC-2	Moodys Branch fm., MS	*Conus tortilis*	38[f]	±1.0[g]	0.45	2.5	3.2	2.1	−0.1	−1.1	0.27	K01	S13
MBT-1	Moodys Branch fm., MS	*Turritella perdita*	38[f]	±1.0[g]	0.02	2.8	3.2	2.4	−0.1	−1.3	0.15	K01	S13
GSC-1	Gosport Sand, AL	*Conus sauridens*	39[f]	±1.0[g]	0.01	2.4	2.7	2.3	−0.7	−1.5	0.13	K01	S13
GST-1	Gosport Sand, AL	*Turritella nasula*	39[f]	±1.0[g]	0.07	3.6	3.8	3.3	0.7	−1.8	0.05	K01	S13
CMT-3	Cook Mountain, MS	*Turritella spp*	40.5[f]	±1.0[g]	0.56	3.1	3.5	2.9	−0.1	−1.1	0.16	K01	S13
CMT-5	Cook Mountain, MS	*Turritella spp*	40.5[f]	±1.0[g]	0.31	2.9	3.1	2.7	0.3	−1.0	0.06	K01	S13
DBC-2	Dobys Bluff fm., MS	*Conus sauridens*	42[f]	±1.0[g]	0.67	2.7	3.0	2.3	−0.5	−2.7	0.08	K01	S13
DBC-4	Dobys Bluff fm., MS	*Conus sauridens*	42[f]	±1.0[g]	0.67	2.6	3.1	2.3	−0.4	−2.1	0.12	K01	S13

[a]Note that *Conus* Sr/Ca data derives from adult growth section (LER > 50 mm/yr). Specimens that show an offset in the timing between the δ^{18}O and Sr/Ca cycles (e.g., MBT-1 and GST-1) are excluded from our interpretations. GOM = Gulf of Mexico, FL = Florida, MS = Mississippi, Al = Alabama, CR = Costa Rica, and PN = Panama.
[b]Ages from *Coates et al.* [1992, 2005].
[c]*Allmon* [1993; revision of age used in *Tao and Grossman*, 2010].
[d]Age estimates from *Coates et al.* [1992] and *Cotton* [1999] updated by W. A. Berggren and M-P. Aubry in *Leon-Rodriguez* [2007].
[e]*Bryant et al.* [1992; revision of age used in *Kobashi et al.*, 2001].
[f]Ages from *Mancini and Tew* [1991] adjusted to the *Berggren et al.* [1995] timescale.
[g]Estimate.
[h]Data sources: K01, *Kobashi et al.* [2001]; S06, *Sosdian et al.* [2006]; G08, *Gentry et al.* [2008]; T10, *Tao and Grossman* [2010]; T12, *Tao* [2012]; S13, this paper; T13, Tao et al. (submitted manuscript, 2012); GUD, E. L. Grossman (unpublished data, 2002); TUD, K. Tao (unpublished data, 2011).

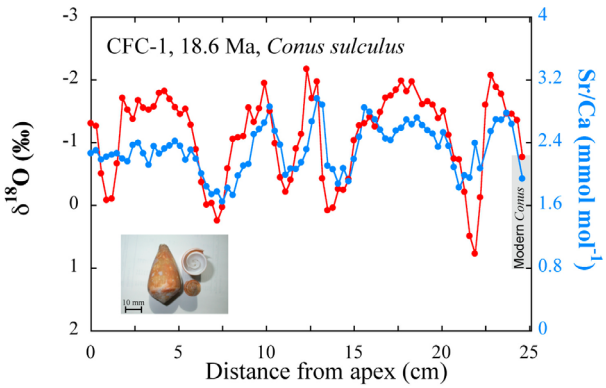

Figure 3. Profiles of Sr/Ca (solid blue circles) and $\delta^{18}O$ (solid red circles) in fossil specimen CFC-1 show strong coherence. Inset picture is a modern *Conus* shell. The shaded box depicts the modern *Conus* shell Sr/Ca range.

respectively [*Tao and Grossman*, 2010; Tao et al., submitted manuscript, 2012], and a Thermo Scientific MAT253 and Kiel IV system for fossil mollusks from Panama and Costa Rica [*Tao*, 2012]. All analyses were calibrated to Vienna-PDB (VPDB) using NBS-19 ($\delta^{18}O$ = -2.20‰). Precision was 0.1‰ or better. Maximum and minimum $\delta^{18}O$ values were used to calculate the total seasonal change in shell $\delta^{18}O$. We assume that the difference is entirely attributable to temperature and apply a temperature-$\delta^{18}O$ sensitivity of 4.2°C per 1‰ [*Grossman and Ku*, 1986]. We then calculate the Sr/Ca-temperature sensitivity by dividing the seasonal Sr/Ca change by the seasonal $\delta^{18}O$-temperature change observed within each shell.

[8] Prior to oxygen isotopic analysis, X-ray diffraction and scanning electron microscopy confirmed that the aragonitic shells were not diagenetically altered. Shells were soaked in water overnight, ultrasonicated in distilled water, and dried at air temperature. If necessary, shells were abraded with sandpaper to remove surface contamination such as iron staining. Sample grooves were milled parallel to growth banding using a 0.3-mm Brasseler carbide drill bit to collect powder samples.

[9] Trace metal analysis was performed by ICP-OES and ICP-MS at Rutgers University, Cardiff University, and TAMU. Aragonite powder splits were progressively reacted with trace metal clean 0.065N HNO_3, until complete dissolution was achieved. After a 10 min centrifugation, 100 μl of the sample solution was further diluted with 300 μl 0.5N HNO_3 to obtain a final Ca concentration of ~4 mM. The long-term precision for Sr/Ca analysis determined by analyzing standards over several years is ±1.5% (RSD).

[10] Sr/Ca_{sw} records from this study and previous publications used in the simple strontium flux model were smoothed using a 60% weighted average curve fit in Kaleidograph. This function fits a curve to the data using the locally weighted least squared error method. Following the smoothing, each Sr/Ca_{sw} record was resampled at 1 Myr sampling resolution before being used as input in the simple model.

3. Results and Discussion

3.1. Temperature Control on Gastropod Sr/Ca

[11] Fossil *Conus* shells show pronounced seasonal Sr/Ca cycles, with a strong inverse correlation between Sr/Ca and $\delta^{18}O$ (R^2 ranges from 0.1 to 0.9, $\rho < 0.05$; Table 1 and Figures 3 and 4). Our fossil turritellids also show similar Sr/Ca cyclicity with significant ($\rho < 0.05$) inverse correlation between Sr/Ca and $\delta^{18}O$ through the seasonal cycles (Figure 5). Modern gastropod Sr/Ca correlates directly with ambient temperature and inversely with shell $\delta^{18}O$ [*Sosdian et al.*, 2006]. Inorganic aragonite exhibits a negative temperature-Sr/Ca relationship, suggesting that the gastropod relationship is driven by kinetic factors. In support of this is the observation by *Tripati et al.* [2009] that slower-growing turritellid species have lower Sr/Ca than faster growing species. However, *Sosdian et al.* [2006] noted that the temperature-driven seasonal variability was superimposed on a long-term ontogenetic trend of increasing Sr/Ca as the shell aged. Because of this ontogenetic effect, *Sosdian et al.* [2006] proposed separate calibrations for juvenile and adult stages of growth in *Conus* shells. Overall, temperature is the primary control on *Conus* and turritellid Sr/Ca variation.

[12] Fossil shell *Conus* and turritellid Sr/Ca values are substantially higher than most modern values (Figure 6a). This difference reflects some combination of warmer temperatures in the mid-Cenozoic [*Zachos et al.*, 1994] and different seawater Sr/Ca. By using appropriate $\delta^{18}O$-Sr/Ca temperature calibrations and partition coefficients it is possible to separate out these two controls on gastropod Sr/Ca [*Sosdian et al.*, 2006; *Tripati et al.*, 2009].

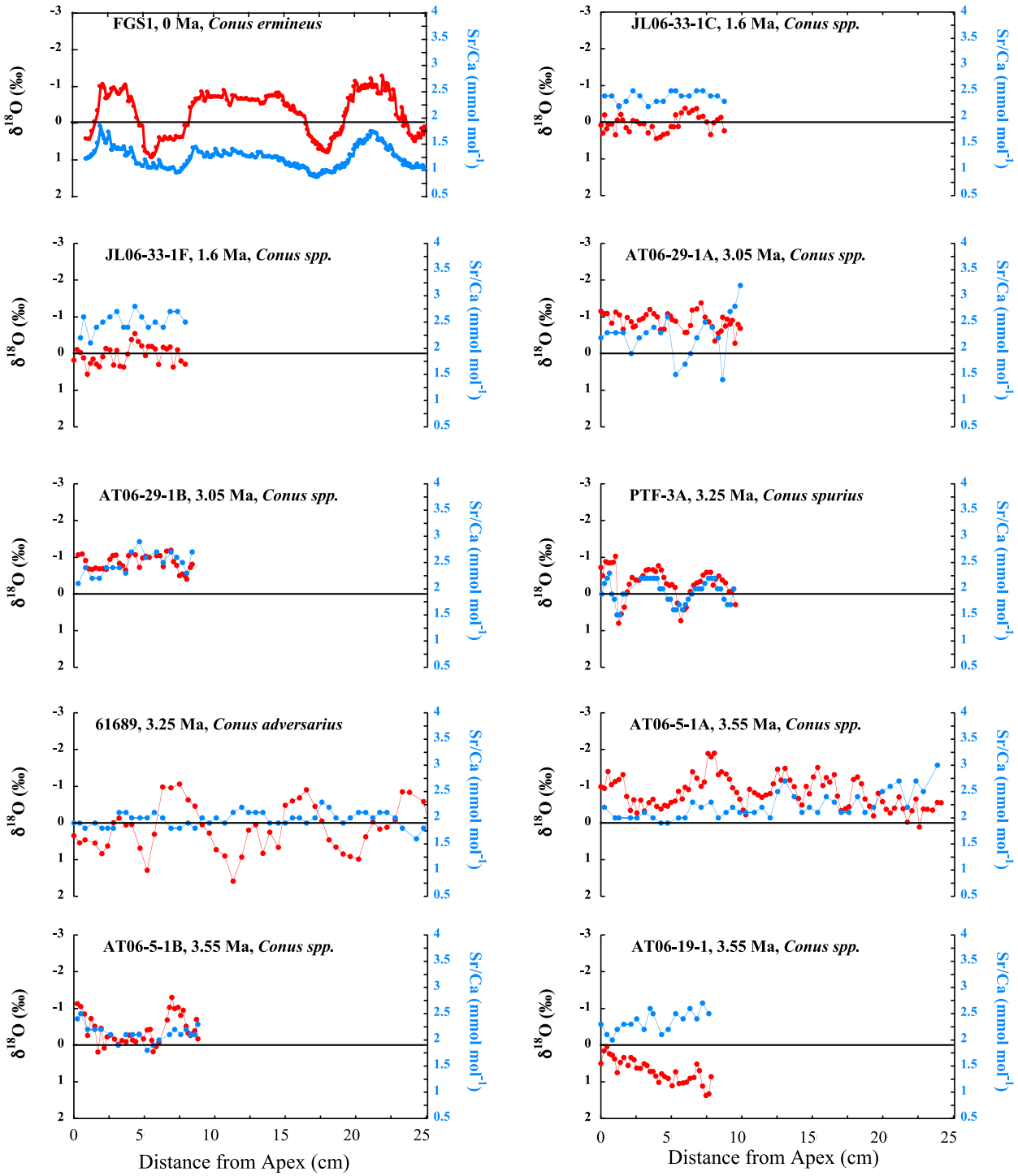

Figure 4. $\delta^{18}O$ and Sr/Ca profiles of *Conus* spp. from modern and fossil specimens. Solid line denotes $\delta^{18}O$ = 0‰ and Sr/Ca = 2 mmol mol^{-1}. See Table 1 for appropriate sources for previously published data.

3.2. Estimating Seawater Sr/Ca

3.2.1. Sr/Ca-Temperature Calibration

[13] The modern adult *Conus ermineus* Sr/Ca-temperature calibration has a slope of 0.072 ± 0.014 (±2 s.e.) mmol mol^{-1} per °C [*Sosdian et al.*, 2006]. The majority of the fossil *Conus* specimens have slow linear extension rates (<50 mm yr^{-1}) as determined using measured length of seasonal profiles, suggesting that this adult calibration is appropriate [*Sosdian et al.*, 2006]. We compared

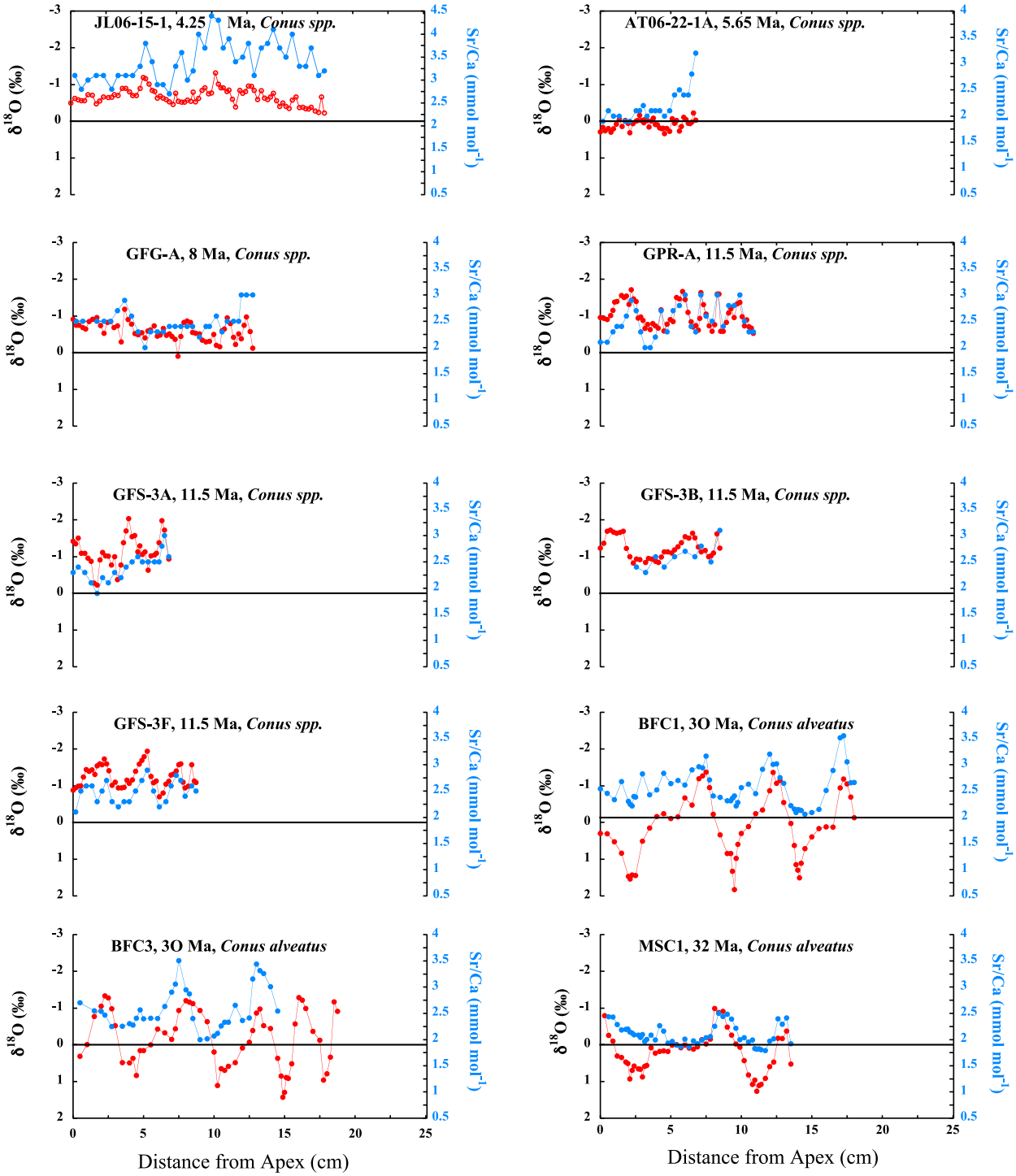

Figure 4. (continued)

the magnitude of the seasonal cycles in $\delta^{18}O$ and Sr/Ca to obtain apparent temperature sensitivities for each shell (see Methods; Table 1). Two fossil specimens (AT06-22-1A and YCC1) yield higher than expected Sr/Ca-temperature sensitivities, likely attributable to site-specific changes in salinity or habitat, and are not considered further. The remaining fossil *Conus* shells produce a range of temperature sensitivities encompassing that of *C. ermineus*, but with a higher mean value (0.15 ± 0.1 (±1 s.d.)

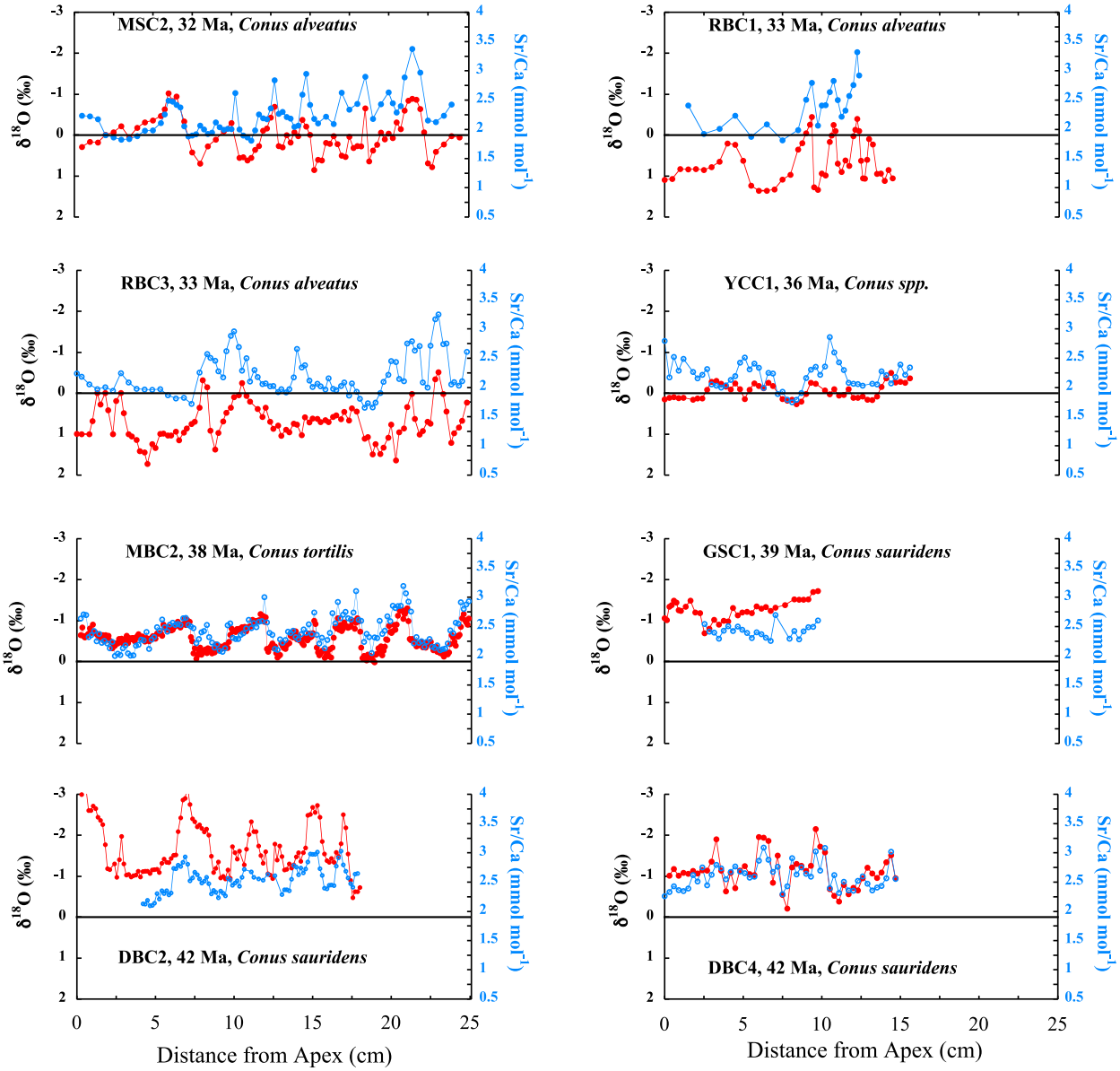

Figure 4. (continued)

mmol mol^{-1} per °C) (Table 1). This range may be primarily due to vital effects (i.e., different species having different temperature sensitivities) and to a lesser extent uncertainties regarding the relative temperature and salinity components of the δ^{18}O profiles. The relatively low apparent temperature sensitivity of the modern calibration species, *Conus ermineus*, may be a result of the shell not growing during temperature extremes. *Gentry et al.* [2008] showed that only 69% of the in situ temperature range is expressed in the δ^{18}O seasonal cycles. The modern Sr/Ca-temperature calibration was calculated using measured instrumental temperature rather than δ^{18}O-temperature and may have underestimated the Sr/Ca temperature dependence [*Sosdian et al.*, 2006]. After re-evaluating the empirical relationship between Sr/Ca and δ^{18}O-temperature cycles in the modern shells from the calibration study [*Sosdian et al.*, 2006], we calculate a higher Sr/Ca-temperature slope (0.089 ± 0.013 (1 s.d.) mmol mol^{-1} per °C, which is closer to the mean temperature sensitivity obtained from the fossil shells. In order to calculate seawater Sr/Ca from the fossil record, we use the mean Sr/Ca-temperature slope derived from the

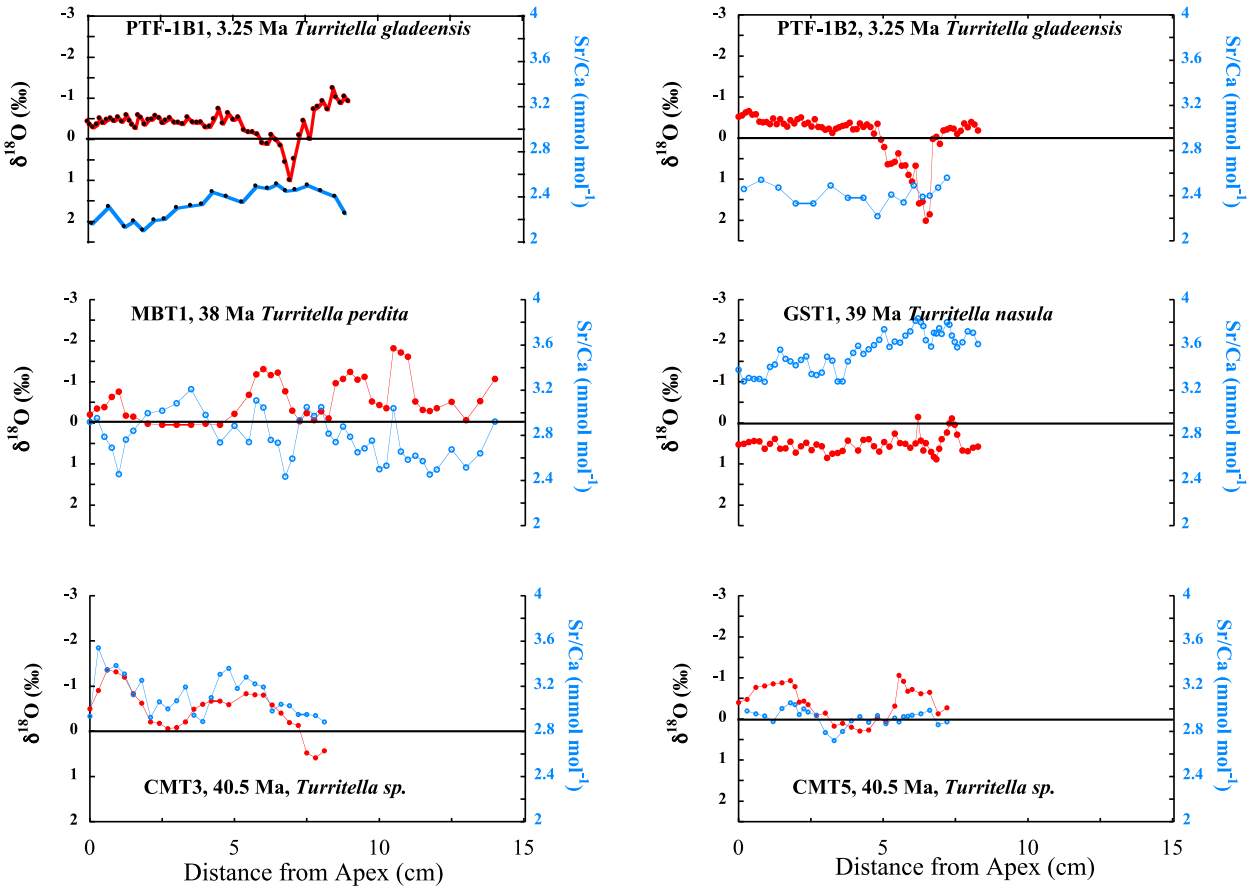

Figure 5. $\delta^{18}O$ and Sr/Ca profiles of turritellids from fossil specimens. Solid line denotes $\delta^{18}O$ = 0‰ and Sr/Ca = 2.9 mmol mol^{-1}. See Table 1 for appropriate sources for previously published data.

fossil specimens (0.15 ± 0.10) and include the 1 s.d. uncertainty envelope in our calculations.

[14] The modern turritellid calibration shows a range of Sr/Ca-temperature sensitivity estimates depending on the species used [*Tripati et al.*, 2009, Figure 2a]. The modern generic turritellid calibration has a Sr/Ca-temperature sensitivity of 0.048 ± 0.009 (2 s.e.) mmol/mol per °C although some species, such as *T. cingulata*, *T. leucostma*, and *M. roseus*, exhibit higher temperature sensitivities (0.08, 0.10, and 0.15 mmol/mol per °C respectively) [*Tripati et al.*, 2009]. An assessment of the Sr/Ca and $\delta^{18}O$-temperature profiles within our six fossil turritellid specimens suggests a relatively high temperature sensitivity (~0.10 ± 0.05 (1 s.d.) mmol mol^{-1} per °C) more similar to these species. We therefore use this sensitivity to reconstruct seawater Sr/Ca from the fossil turritellid shell Sr/Ca record. Further work evaluating both the *Conus* and turritellid species-specific Sr/Ca-temperature relationships would reduce the large error envelope on the seawater Sr/Ca estimates.

3.2.2. Interspecific Offsets

[15] The large range in absolute Sr/Ca within the eleven modern *Conus* species indicates the presence of vital effects, i.e., interspecific offsets in the strontium distribution coefficient (D_{Sr}) at a given temperature (Figure 6a). One way to correct for such vital effects is to construct a record of gastropod Sr/Ca using temporally overlapping species. However, this has not been possible with our samples. Therefore, our approach here is to normalize all *Conus* Sr/Ca to a constant temperature (Figure 6b), and then use the mean distribution coefficient determined from the eleven modern species to estimate seawater Sr/Ca (equation (1)) (Figure 6c). In order to normalize the shell Sr/Ca to a given temperature (30°C) we estimated seawater temperature from the $\delta^{18}O$ of the same shell [*Kobashi et al.*,

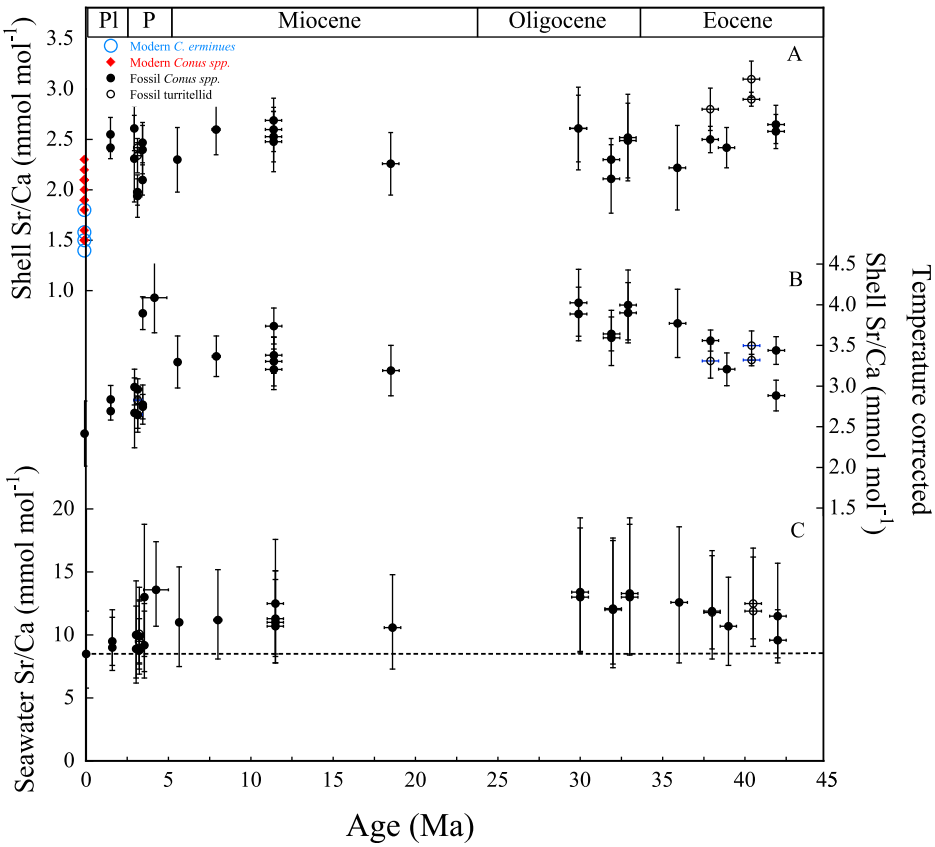

Figure 6. (a) Shell Sr/Ca for modern *Conus* spp. specimens and Cenozoic turritellid and *Conus* specimens. Modern *Conus ermineus* (blue open circles) were used to construct the Sr/Ca-temperature calibration [*Sosdian et al.*, 2006]. Data from other modern *Conus* species (red circles) are included to evaluate inter-species offsets. (b) *Conus* and turritellid shell Sr/Ca corrected to 30°C using the temperature sensitivity, 0.15 ± 0.1 mmol/mol per °C and 0.10 ± 0.5, respectively) derived from fossil *Conus spp.* and turritellids; (c) Sr/Ca_{sw} estimates from this study. The temperature corrected Sr/Ca record (Figure 6b) was converted to Sr/Ca_{sw} using the mean D_{Sr} (=0.30 ± 0.05 and 0.31 ± 0.05) determined from the modern *Conus* and turritellid specimens. P = Pliocene and Pl = Pleistocene in the highlighted epochs. Dashed line represents the modern-day value of Sr/Ca_{sw}.

2001; Tao et al., submitted manuscript, 2012] using the *Grossman and Ku* [1986] (equation (1)) paleotemperature equation.

[16] Miocene seawater $\delta^{18}O$ was determined using estimates from *Lear et al.* [2000] corrected for paleo-latitude following *Zachos et al.* [1994]. Pliocene seawater $\delta^{18}O$ estimates are from *Williams et al.* [2009] and glacial Pleistocene seawater $\delta^{18}O$ estimates are from *Schmidt et al.* [2004].

$$Sr/Ca_{sw} = \text{Temperature corrected } (Sr/Ca)_{shell}/D_{Sr@30°C} \quad (1)$$

The value of D_{Sr} at 30°C was calculated using modern shell Sr/Ca and assuming modern Sr/Ca_{sw} of 8.54 mmol/mol [*de Villiers*, 1999]. The modern temperature calibration species *Conus ermineus* has an average Sr/Ca value of 1.5 mmol/mol, which corresponds to a D_{Sr} of 0.23 at 30°C. *Conus mus* has a mean Sr/Ca = 1.6 mmol/mol (D_{Sr} = 0.19 at 30°C), the other modern *Conus* species (*C. jaspideus, C. recurvus, C. mahogani, C. arcuatus, C. patricius, C. ximenes, and C. floridanus*) have substantially higher Sr/Ca values (ranging from 1.8 to 2.3 mmol/mol), corresponding to a range in D_{Sr} of 0.26 to 0.34 at 30°C. Here we use a mean value of D_{Sr} = 0.30 ± 0.05 (1 s.d.) at 30°C to calculate Cenozoic seawater Sr/Ca from *Conus* Sr/Ca (equation (1)). For our turritellid gastropods we use a D_{Sr} of 0.31 ± 0.05 (1 s.d.) at 30°C determined from the modern turritellid calibration [*Tripati et al.*, 2009]. We use the range in modern *Conus* D_{Sr} to estimate the associated uncertainties in our reconstructed seawater Sr/Ca through the Cenozoic.

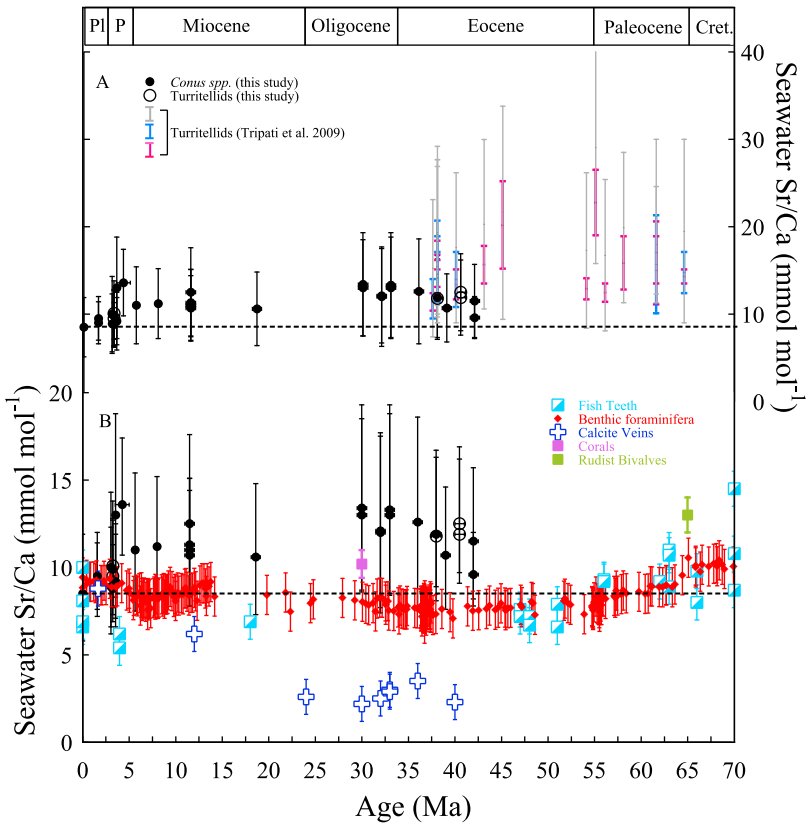

Figure 7. (a) Seawater Sr/Ca estimates from *Conus* and turritellid gastropods (this study) compared to the estimates from *Tripati et al.* [2009] based on turritellid gastropods. Error bars for the seawater Sr/Ca estimates from this study represent ±1 s.d. of both the D_{Sr} and temperature sensitivity. Error bars for the *Tripati et al.* [2009] study represent a range of seawater Sr/Ca estimates (see Table 3 in *Tripati et al.* [2009] for details) calculated using a D_{Sr} range of 0.13 to 0.31 (red error bars) and using D_{Sr}-temperature relationship determined from modern Turritellidae (blue error bars) and modern *T. exoleta* (gray error bars; see Table 3 in *Tripati et al.* [2009] for details). (b) Compilation of reconstructed seawater Sr/Ca records for the last 65 million years. Data are from calcite veins [*Coggon et al.*, 2010], benthic foraminifera [*Lear et al.*, 2003], fossil fish teeth [*Balter et al.*, 2011], corals [*Ivany et al.*, 2004], and rudists bivalves [*Steuber and Veizer*, 2002]. Error bars for the calcite veins, fish teeth, corals, and rudist/belemnites proxy records are derived from the referenced literature. Error bars for the benthic foraminifera record represent the average 2 s.d. (=0.56 mmol/mol) of the 97 time intervals where more than one data point was present. P = Pliocene, Pl = Pleistocene and Cret. = Cretaceous in the highlighted epochs. Dashed line represents the modern-day value of Sr/Ca_{sw}.

[17] Our new gastropod seawater Sr/Ca record overlaps with the record of *Tripati et al.* [2009] derived using Eocene turritellids (Figure 7a), allowing direct comparison. The larger variability in the *Tripati et al.* [2009] data reflects the lack of $\delta^{18}O$-temperature estimates for most of the shells, and uncertainties associated with interspecies vital effects and temperature sensitivities. When combined, these uncertainties produce a wide range of reconstructed seawater Sr/Ca for each of the turritellid shells from the *Tripati et al.* [2009] data set (Figure 7a). Therefore, while our turritellid shell Sr/Ca record is similar to the *Tripati et al.* [2009] shell record, our reconstructed seawater Sr/Ca ratios derived from shells, for which we apply specimen-based $\delta^{18}O$ temperature corrections, a higher Sr/Ca-temperature sensitivity, and interspecies corrections, fall at the extreme lower end of the *Tripati et al.* [2009] estimates. Reassuringly, our turritellid-based seawater Sr/Ca estimates are within error of our contemporaneous *Conus*-based record (Figure 6c).

3.2.3. Cenozoic Sr/Ca_{sw} Variations

[18] Our combined *Conus* and turritellid Sr/Ca_{sw} record suggests minimal change in seawater Sr/Ca across the Eocene to the Pliocene given the uncertainty in the Sr/Ca_{sw} calculations. The Sr/Ca_{sw} record

variability is close to the calibration errors of the proxy (i.e., 1 s.d. on modern D_{Sr} at 30°C calculated using a range of modern *Conus* and turritellid species and 1 s.d. on the Sr/Ca-temperature slope for each genus). Nevertheless, the gastropod record does indicate that seawater Sr/Ca has not varied by more than ~50% for the last 42 Ma (Figure 6c). Our record is in good agreement with several other proxies. For example, coral Sr/Ca suggests that Oligocene Sr/Ca_{sw} was ~10 mmol/mol, in excellent agreement with our gastropod based reconstruction [*Ivany et al.*, 2004]. Sr/Ca ratios in marine barite indicate that Sr/Ca_{sw} exhibited higher than modern values in the Miocene similar to our findings (Figure 7b) [*Averyt and Paytan*, 2002]. Other records are consistent with a secular trend of declining Sr/Ca_{sw} through time. For example, Sr/Ca measurements of belemnites and molluscs indicate high Sr/Ca_{sw} in the Cretaceous (~13–14 mmol/mol) [*Steuber and Veizer*, 2002], although this value depends heavily on the choice of D_{Sr}. The strontium content of marine cements implies that late Cretaceous seawater [Sr] was at least twice that of Quaternary seawater (i.e. >16 mmol/mol) [*Opdyke et al.*, 1995].

[19] Our Eocene Sr/Ca_{sw} estimates (11.4 ± 3 mmol/mol (1 s.d.)) at 36–42 Ma are significantly higher than estimates based on Cenozoic planktonic foraminifera [7 mmol/mol; *Graham et al.*, 1982], benthic foraminifera [7.7 mmol/mol; *Lear et al.*, 2003] and fossil fish teeth enamel (7.2 mmol/mol [*Balter et al.*, 2011]) (Figure 7b). Interpretation of the planktonic foraminiferal Sr/Ca record is limited due to considerable scatter, use of multiple species, and uncertain controls on foraminiferal Sr/Ca [*Elderfield et al.*, 2002; *Dueñas-Bohórquez et al.*, 2009]. *Lear et al.* [2003] observed a small decrease in modern and fossil benthic foraminiferal Sr/Ca with increasing water depth on the order of 10% per km, which has been partially attributed to saturation effects [*Elderfield et al.*, 1996; *Rosenthal et al.*, 1997; *Dueñas-Bohórquez et al.*, 2011]. Proxy records highlight a potential increase in carbonate saturation from the mid-Eocene to early Oligocene [*Lear and Rosenthal*, 2006]. Such an increase would drive benthic foraminiferal derived Sr/Ca_{sw} estimates closer to the gastropod derived Sr/Ca_{sw} estimates but changing carbonate saturation levels were unlikely large enough to explain the entire difference. Recent studies suggest that interpretation of Sr/Ca_{sw} reconstructions derived from fossil fish teeth may be complicated by changes in the relative contributions of different food sources (e.g., a 15% change in [Sr] is evident in bones at each trophic step) [*Balter*, 2004; *Balter and Lécuyer*, 2010]. *Balter et al.* [2011] suggest that these dietary effects can explain part of the observed variability in the different taxa analyzed in their study. For example, modern Sr/Ca_{sw} values derived from sharks and rays range from 6.75 mmol/mol to 9.05 mmol/mol, respectively [*Balter et al.*, 2011]. While the various biogenic proxy records for Cenozoic Sr/Ca_{sw} show significant differences reflecting the uncertainties discussed above (Figure 7b), they all show substantially higher Sr/Ca_{sw} than the record derived from mid-ocean ridge CCVs (~2 mmol/mol at 40 Ma) [*Coggon et al.*, 2010].

[20] The potential bias in the CCV Sr/Ca_{sw} record could be related to the uncertainties in the proxy assumptions and constraints. The Neogene CCV Sr/Ca_{sw} reconstruction shows strong covariance with the corresponding CCV Mg/Ca_{sw} record [*Coggon et al.*, 2010]. This has been interpreted as reflecting constant Sr/Mg_{sw} [*Coggon et al.*, 2010, 2011]. However, D_{Sr} for calcite is strongly dependent on Mg content [*Mucci and Morse*, 1983; *Carpenter and Lohmann*, 1992; *Broecker and Yu*, 2011]. Additionally, the CCV Sr/Ca_{sw} reconstructions depend on an accurate estimate of the degree of fluid evolution prior to calcite precipitation. $^{87}Sr/^{86}Sr$ – Sr/Ca crossplots from the "hot-water" hydrothermal system suggest that the slope of the Sr/Ca-$^{87}Sr/^{86}Sr$ relationship is steeper at lower temperatures [*Coggon et al.*, 2010]. The CCVs used to reconstruct the low seawater Sr/Ca ratios for the Paleogene were formed in "cold-water" systems assuming no geochemical fluid evolution prior to calcite precipitation. Allowing for even a small degree of fluid evolution prior to precipitation of these CCVs might raise the reconstructed seawater Sr/Ca values closer to our gastropod record. Finally, we note that the increasing trend in seawater Sr/Ca from the late Eocene to present, as deduced from the CCV records, seems at odds with the general covariance between seawater Sr/Ca and the transition from calcite to aragonite seas during the Phanerozoic proposed by *Steuber and Veizer* [2002]. Based on that record, one would expect a decrease in seawater Sr/Ca with increasing proportion of aragonite deposits, consistent with the secular decrease from the mid Cretaceous.

[21] In the following discussion, we examine the long-term trends in Sr/Ca_{sw} records derived from biogenic proxies (i.e., gastropod, benthic foraminifera, and fossil fish teeth) and inorganic precipitates (i.e., calcite veins) to test the plausibility of the various geological scenarios inferred by each reconstruction. The coral, rudist, and belemnite records are of too low resolution to be included in this analysis. The gastropod record reconstructed in this study is

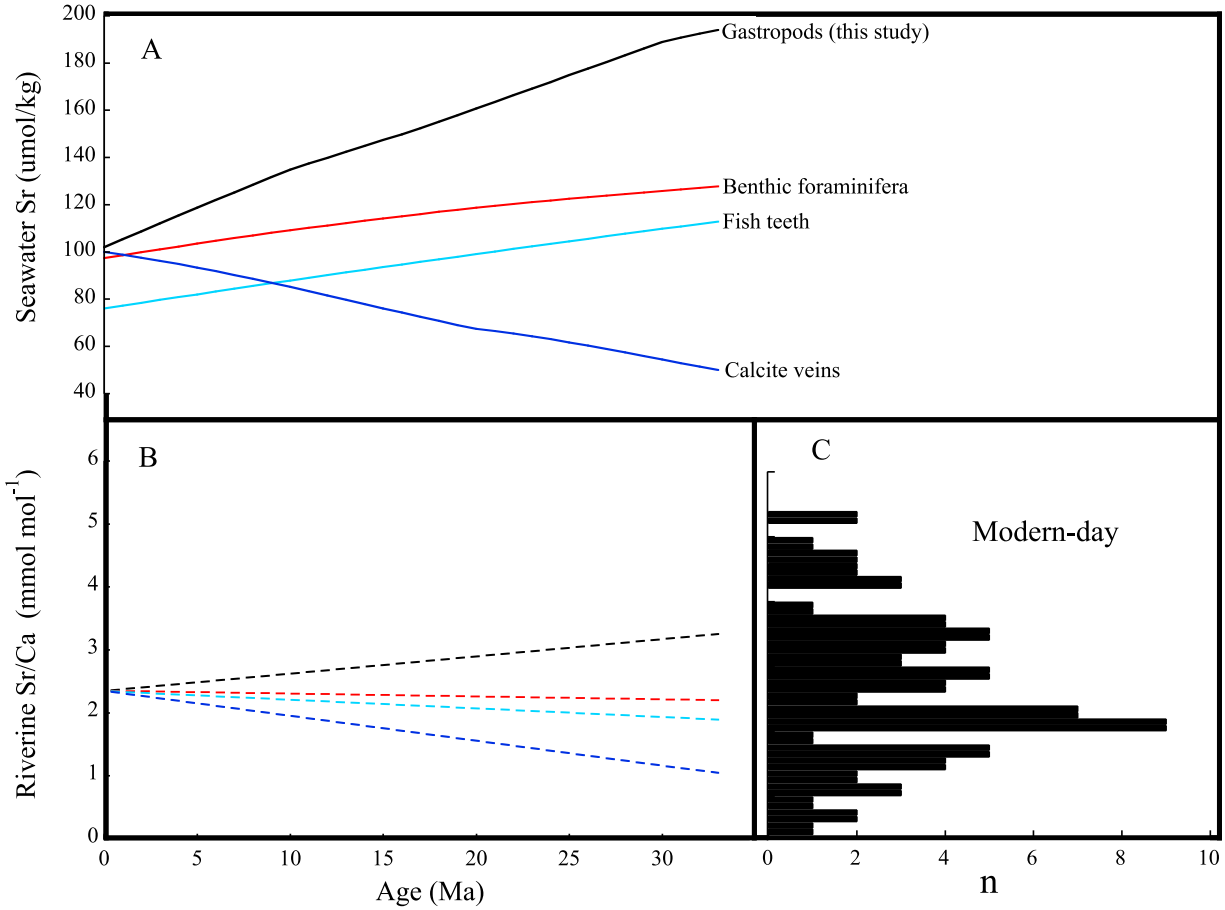

Figure 8. (a) Estimated seawater Sr^{2+} concentrations based on benthic foraminifera, fossil fish teeth, CCVs, and gastropod Sr/Ca measurements from this study using the [Ca] record from *Horita et al.* [2002] (Figure S1 in Text S1 in the auxiliary material). Trendlines are 60% weighted averages for each data set. (b) Calculated riverine Sr/Ca (mol/mol) based on benthic foraminifera, fossil fish teeth, CCVs, and gastropod Sr/Ca measurements assuming a constant rate of change between the modeled 33 Ma value (see text) and modern average value of 2.35 mmol/mol [*Meybeck and Ragu*, 1996; *Holmden et al.*, 1997; *Gaillardet et al.*, 1999; *Vance et al.*, 2009]. (c) Range of modern day riverine Sr/Ca based on discharge weighted average river composition shown in a histogram (n equals number of rivers [*Meybeck and Ragu*, 1996; *Holmden et al.*, 1997; *Gaillardet et al.*, 1999; *Vance et al.*, 2009]).

not spliced with the *Tripati et al.* [2009] gastropod Sr/Ca_{sw} record for reasons described earlier.

3.3. Controls on Cenozoic Sr/Ca_{sw} Variations

[22] Strontium and calcium are major ions in seawater with relatively long residence times, 2.5–3 Myr and 1 Myr, respectively [*Broecker and Peng*, 1982; *Palmer and Edmond*, 1989]. Seawater Sr/Ca is controlled by the balance between input and removal processes for Ca and Sr and could be modified by a change in either [Sr] or [Ca] or both. The major source of both Sr^{2+} and Ca^{2+} to the oceans is continental weathering, whereas hydrothermal exchange can be an important source for Ca^{2+} while insignificant for Sr^{2+} [*Elderfield and Schultz*, 1996]. Carbonate sedimentation is a major sink for Ca and Sr, with a relative flux that depends on the mass and mineralogy of the accumulating sediments. Predominant calcite deposition (D_{Sr} ~0.1) would increase seawater Sr/Ca, whereas predominant aragonite deposition (D_{Sr} ~1) would have a minor effect on seawater Sr/Ca if all other variables were held constant [*Stoll and Schrag*, 1998].

[23] Secular variations in seawater [Ca] have been derived from chemical analyses (e.g., fluid inclusions, Ca isotopes) and mass balance modeling. All techniques show that seawater [Ca] progressively decreased through the Cenozoic [*Hardie*, 1996; *Stanley and Hardie*, 1998; *De La Rocha and DePaolo*, 2000;

Lowenstein et al., 2001; *Horita et al.*, 2002]. Using the fluid inclusion [Ca] record [*Horita et al.*, 2002] (Figure S1 in Text S1 in the auxiliary material), we calculate Cenozoic seawater [Sr] for each of the four Sr/Ca_{sw} proxy records (Figure 8a).[1] We smoothed all of the Sr/Ca records in the same manner (using a 60% weighted average of each Sr/Ca record) to minimize artifacts owing to sampling resolution. The benthic foraminiferal, fish teeth, and gastropod seawater [Sr] records show similar trends but of different magnitude, whereas the CCV [Sr] record shows a markedly different trend (Figure 8a). The largest discrepancy between the [Sr] records occurs in the Neogene: the gastropod, benthic foraminifera, and fish teeth records imply decreasing seawater [Sr] whereas the CCV record implies increasing [Sr] through the Neogene (Figure 8a).

3.4. Strontium Flux Model

[24] Changes in seawater [Sr] can be expressed as:

$$dSr/dt = JSr_{RIV} - Sr/Ca_{sw} \cdot JCa_{PELAGIC} \cdot DSr_{PELAGIC} - Sr/Ca_{sw} \cdot JCa_{SHELF} \cdot DSr_{SHELF} \quad (2)$$

where JSr_{RIV} is riverine flux of Sr^{2+}, $JCa_{PELAGIC}$ and JCa_{SHELF} are the Ca fluxes into marine carbonates and $DSr_{PELAGIC}$ and DSr_{SHELF} are the corresponding average strontium distribution coefficients. The exposure of shelf aragonite during sea level falls and subsequent recrystallization releases Sr into the ocean. *Stoll and Schrag* [1998] used a modeling study to show that Quaternary sea level variations resulted in only a 1–3% change in Sr/Ca_{sw}. Thus the predicted change in Sr/Ca_{sw} due to recrystallization is small relative to the change observed in the Cenozoic Sr/Ca_{sw} records and therefore was not included in our simple model. Using tabulated pelagic and shelf carbonate depositional fluxes from *Opdyke and Wilkinson* [1988] (Figure S2 in Text S1 in the auxiliary material) and modified Pliocene to Quaternary estimates from *Nakamori* [2001] and a constant value of 0.1 for $DSr_{PELAGIC}$ (assuming pelagic carbonate deposition to be dominated by calcite), equation (2) can be solved for riverine Sr^{2+} flux or DSr_{SHELF} if assumptions are made regarding one of these parameters.

3.5. Estimating Global Average Riverine Sr/Ca

[25] Here we evaluate whether any of the seawater Sr/Ca reconstructions could be explained by realistic changes in the riverine Sr/Ca through time. We use each seawater Sr/Ca proxy record to estimate riverine Sr/Ca at 33 Ma, and then compare the results with the modern range of Sr/Ca values measured from rivers draining a wide variety of catchment types (e.g., carbonate-dominated bedrock versus silicate dominated bedrock). The riverine Sr/Ca ratio is estimated by calculating JSr_{RIV} and JCa_{RIV} separately, using the rate of change in seawater [Sr] and [Ca] inferred from the smoothed records over a 1 million year interval at 33 Ma and equations (2) and (3).

$$JCa_{RIV} = dCa/dt - JCa_{HYDRO} + JCa_{PELAGIC} + JCa_{SHELF} \quad (3)$$

where JCa_{RIV} is the riverine flux of Ca^{2+}, JCa_{HYDRO} is the hydrothermal flux of Ca^{2+}, and dCa/dt is the change in seawater [Ca] record of *Horita et al.* [2002] (Figure S1a in Text S1 in the auxiliary material).

[26] We chose 33 Ma as an interval to estimate riverine Sr/Ca because equation (3) includes a [Ca] hydrothermal flux term, and several published estimates of oceanic crustal production agree that the rate at this time was similar (~10% higher) to that of today [*Berner*, 1994; *Conrad and Lithgow-Bertelloni*, 2007; *Müller et al.*, 2008] (Figure S3a in Text S1 in the auxiliary material). We therefore used a hydrothermal Ca flux ~10% higher than the modern day estimate of 1.85×10^{12} mol/yr from *Elderfield and Schultz* [1996], which includes estimates from mid-ocean ridges and ridge flanks. To calculate JSr_{RIV} at 33 Ma we used equation (2) and assumed DSr_{SHELF} was 0.3. This value is equivalent to a ~3:1 proportion of calcite to aragonite in shelf carbonates (using ball-park values of 1.0 and 0.1 for aragonite and calcite D_{Sr} respectively), which is consistent with a reduction in the number of aragonite-dominated reef sites in the early Oligocene relative to today [*Kiessling* 2009] (Figure 9). Having estimated riverine Sr/Ca at 33 Ma, we then assumed a constant rate of change of riverine Sr/Ca between 33 Ma and today (modern average river Sr/Ca = 2.35 mmol/mol) for each seawater Sr/Ca scenario (Figure 8b). In the following discussion, we evaluate riverine Sr/Ca estimates derived from each Sr/Ca_{sw} record in light of the modern-day range of riverine Sr/Ca.

3.6. Evaluating Estimates of Past Riverine Sr/Ca

[27] Past changes in the global composition of river discharge are difficult to quantify but most likely varied within the modern range of present-day major rivers, which span a wide variety of

[1] Auxiliary materials are available in the HTML. doi:10.1029/2012GC004240.

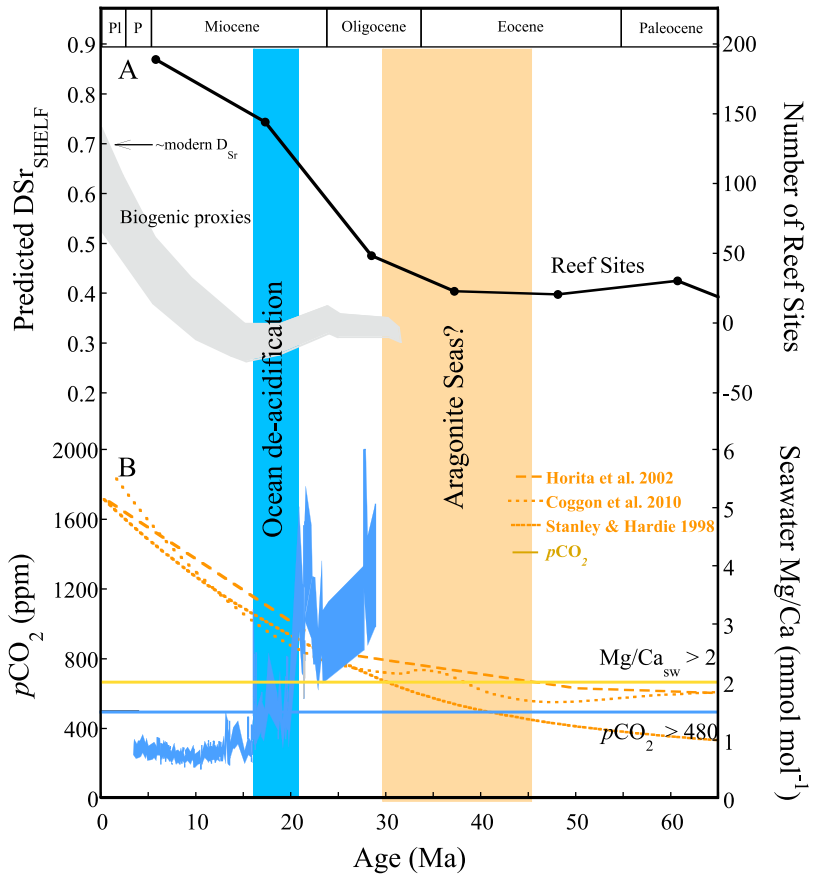

Figure 9. (a) Estimated number of reef sites (black line) [*Kiessling*, 2009] and calculated D_{Sr} for shelf carbonates based on biogenic proxy estimates (benthic foraminifera and fossil fish teeth) of Sr/Ca_{sw} (gray shaded region). (b) Atmospheric carbon dioxide concentrations from *Pagani et al.* [2005] (blue shaded area), seawater Mg/Ca estimates from fluid inclusions in marine halites [*Horita et al.*, 2002], CCVs [*Coggon et al.*, 2010] and modeling [*Stanley and Hardie*, 1998]. Horizontal orange bar is the aragonite seas Mg/Ca threshold (~2 mol/mol) [*Stanley and Hardie*, 1998], horizontal blue bar marks the CO_2 threshold for the success of coral reef communities (~480 ppm) [*Hoegh-Guldberg et al.*, 2007]. Arrow denotes average modern DSr_{SHELF} values as determined from percentage of aragonite and other calcites in modern shelf environments and their corresponding average strontium distribution coefficients [*Land*, 1967; *Kinsman and Holland*, 1969; *Katz et al.*, 1972].

catchment types. Sr/Ca ratios of the discharge-weighted average river composition of most modern rivers vary between 0.5 and 6 mmol/mol, with an average of 2.35 mmol/mol (Figure 8c) [*Meybeck and Ragu*, 1996; *Holmden et al.*, 1997; *Gaillardet et al.*, 1999; *Vance et al.*, 2009]. The gastropod, benthic foraminifera, fish teeth and CCV records produce riverine Sr/Ca estimates that are respectively 40% higher, 10% lower, 20% lower, and 60% lower at 33 Ma relative to today (Figure 8c). The riverine Sr/Ca estimates derived from the gastropod and CCV records fall in the 80th and 10th percentiles of the tabulated modern range, whereas the benthic foraminifera and fish teeth fall within the 50th and 40th percentiles [*Meybeck and Ragu*, 1996; *Holmden et al.*, 1997; *Gaillardet et al.*, 1999; *Vance et al.*, 2009]. Our uncertainty envelope in the gastropod-derived Sr/Ca_{sw} estimates is ±3 mmol/mol and the lower edge of this envelope falls within 10% of modern average riverine Sr/Ca.

[28] Temporal variability in the Sr/Ca ratio of riverine input could be related to the differing proportions of silicate weathering (i.e., high Sr/Ca ratios) to carbonate weathering (i.e., low Sr/Ca ratios) in the catchment areas [*Gaillardet et al.*, 1999; *Gibbs et al.*, 1999]. In the modern-day, carbonates dominate the material weathered with silicates representing a smaller component of the global fluxes [*Gaillardet et al.*, 1999]. Paleogeographic maps documenting changes in the dominant composition of catchments for every period through the Phanerozoic [*Bluth and Kump*, 1991] show that carbonate bedrock

dominated the catchment lithologies in the mid-Cenozoic as it does today and that there was minimal variation with time in the dominant lithologies in the source areas, albeit the maps are of low resolution [*Bluth and Kump*, 1991]. Therefore, our riverine Sr/Ca reconstructions suggest that the seawater Sr/Ca histories derived from the biogenic carbonate-based proxies (benthic foraminifera, fish teeth and the lower bound of the gastropod Sr/Ca_{sw} record) all appear reasonable (i.e., within the collective range of most modern rivers) given our current understanding of Sr and Ca cycling but that the controls on the CCV Sr/Ca record are not yet fully understood. We note, however, that further investigation of the inter-species offsets, temperature sensitivity, and vital effects of modern *Conus* and turritellid species are necessary to narrow the range of Sr/Ca_{sw} estimates and critically examine the gastropod Sr/Ca_{sw} proxy.

[29] We also acknowledge that the robustness of these riverine Sr/Ca estimates is dependent on the parameterization of JCa_{HYDRO}. Uncertainties in the magnitude of the modern hydrothermal flux of calcium from mid-ocean ridges and flanks produce a wide range of modern JCa_{HYDRO} estimates from 2.1×10^{11} mol/yr to 6.3×10^{12} mol/yr [*Edmond et al.*, 1979; *Berner and Berner*, 1996; *Elderfield and Schultz*, 1996; *Alt*, 2003; *DePaolo*, 2004]. The JCa_{HYDRO} flux used here (that of *Elderfield and Schultz* [1996]) is the most comprehensive estimate within the available published range considering estimates of the modern oceanic calcium budget. Therefore we consider this a preliminary assessment, which can be revisited once estimates of the global hydrothermal calcium flux are refined. As such, our suggestion that the CCV seawater Sr/Ca record is unreasonable should be considered tentative, although the general coherence between the biogenic calcite, aragonite and apatite proxies supports this view.

3.7. Seawater Sr/Ca and Evolution of Cenozoic Aragonite Deposition

[30] Global average DSr_{SHELF} is controlled by the relative proportions of aragonite, calcite and high-Mg calcite deposition in shelf carbonates. Therefore, changes in DSr_{SHELF} through time reflect global trends in the evolution of carbonate-secreting organisms. Here we use the seawater Sr/Ca records derived from two biogenic proxies (benthic foraminifera and fish teeth) in conjunction with equations (2) and (3) to estimate DSr_{SHELF} between 33 Ma and today (Figure 9). We use the pelagic and shelf carbonate depositional fluxes tabulated by *Opdyke and Wilkinson* [1988] and modified by *Nakamori* [2001] and assume that pelagic carbonates were dominated by calcite deposition throughout the Cenozoic ($DSr_{PELAGIC} = 0.1$). As before, JCa_{RIV} was determined using equation (3) assuming hydrothermal Ca flux was 10% higher than modern at 33 Ma and linearly decreased to modern values, and JSr_{RIV} was calculated using JCa_{RIV} and our record of global average riverine Sr/Ca, which assumes an initial value of 0.3 for DSr_{SHELF} at 33 Ma (Figure 8b). The main uncertainties in our model parameters are the assumption that hydrothermal activity decreased linearly between 33 Ma and today, the modern estimate of JCa_{HYDRO} and the riverine Sr/Ca estimates. Several experiments were therefore performed to assess the sensitivity of our calculated record of DSr_{SHELF} to these input parameters (Figures S3–S5 in Text S1 in the auxiliary material). In order to assess how the various hydrothermal flux trajectories affect our estimates of DSr_{SHELF} we followed *Berner* [1994] and assumed that global ocean crustal production rate and hydrothermal calcium flux are linearly scaled (equation (4)).

$$\text{Crustal production-t/Crustal production-0} = JCa_{HYDRO}\text{-t}/JCa_{HYDRO}\text{-0} \quad (4)$$

where t = time in model and 0 = present-day. For JCa_{HYDRO}-0 we use 1.85×10^{12} mol/yr [*Elderfield and Schultz*, 1996], for crustal production-t between 33 Ma and today we compared three published scenarios [*Berner*, 1994; *Conrad and Lithgow-Bertelloni*, 2007; *Müller et al.*, 2008] (Figure S3 in Text S1 in the auxiliary material). Our overall trend in calculated DSr_{SHELF} is unaffected by choice of crustal production scenario (i.e., the left hand side of equation (4)) (Figure S3 in Text S1 in the auxiliary material). We assessed separately the impact of the total hydrothermal calcium flux (i.e., the right hand side of equation (4)) by using different values for JCa_{HYDRO}-0 (Figure S4 in Text S1 in the auxiliary material). We found that the overall trend in predicted DSr_{SHELF} does not vary with various estimates of [Ca] hydrothermal flux but rather the absolute values of the modern DSr_{SHELF} decreases with higher estimates of [Ca] hydrothermal flux. In order to assess the sensitivity of our DSr_{SHELF} estimates to riverine Sr/Ca we compared two scenarios. In the first we used modern riverine Sr/Ca values throughout the modeled interval (33–0 Ma), and in the second we used the appropriate riverine Sr/Ca record from Figure 8b based on the relevant proxy method (i.e., benthic foraminifera or fish teeth). The

first scenario produces DSr_{SHELF} values approximately 25% higher than the second scenario at 33 Ma, with the offset between the scenarios diminishing to zero for the present-day (Figure S5 in Text S1 in the auxiliary material). The overall trend in calculated DSr_{SHELF} is not affected by choice of riverine Sr/Ca history (Figure S5 in Text S1 in the auxiliary material).

[31] Taking the above uncertainties into account, both the benthic foraminifera record and the fish teeth record suggest that DSr_{SHELF} was relatively constant through the mid-Cenozoic, followed by a long-term increase in the proportion of aragonite to calcite deposition beginning in the Miocene (Figure 9a). As expected from Figure 7, the lower bound of the gastropod derived Sr/Ca_{sw} record produces a DSr_{SHELF} record that is very similar to the record derived from benthic foraminifera. At first sight, the sharp increase in DSr_{SHELF} in the middle Miocene (Figure 9) may seem unexpected, given the relatively flat nature of the various seawater Sr/Ca proxy records at this time (Figure 7). The increase in DSr_{SHELF} is driven by the dramatic increase in the pelagic carbonate sedimentation in the middle Miocene [*Opdyke and Wilkinson*, 1988] (Figure S2 in Text S1 in the auxiliary material). All else being equal, because $DSr_{PELAGIC} \ll 1$, such a change in ocean calcium and strontium cycling would tend to increase seawater Sr/Ca. Therefore, in order to balance this model input and produce the trends of decreasing seawater [Sr] seen in Figure 8, the model increases the flux of strontium leaving the ocean by increasing DSr_{SHELF}.

[32] We interpret our DSr_{SHELF} record as representing a long-term increase in the proportion of aragonite to calcite deposition that began in the Miocene (Figure 9a). The overall trend of our DSr_{SHELF} record bears some similarities with a record of coral reef site abundance [*Kiessling*, 2009] (Figure 9a), with the most dramatic increase in reef sites occurring between the late Oligocene and early to mid-Miocene. The rise to dominance of some aragonite-secreting organisms has been attributed to seawater Mg/Ca increasing above a threshold of ~2 mol/mol, with the dependence of aragonite saturation state on seawater carbonate chemistry being assigned a lesser role [*Stanley and Hardie*, 1998]. Most seawater Mg/Ca proxy records (fluid inclusions, CCVs, echinoderms) suggest that this threshold was passed in the mid-Eocene to early Oligocene (44 to 30 Ma) [*Lowenstein et al.*, 2001; *Dickson*, 2002; *Horita et al.*, 2002; *Coggon et al.*, 2010] with a few others suggesting it was passed even earlier [*Lear et al.*, 2002; *Broecker and Yu*, 2011], prior to the dramatic rise in the reef site record (Figure 9).

[33] In addition to Mg/Ca ratio, carbonate saturation may be an important influence on marine calcification. It has recently been shown that atmospheric carbon dioxide concentrations (pCO_2) above 480 ppm might hinder the calcification of aragonitic coral skeletons, and thus coral reefs, by increasing surface ocean acidity and decreasing seawater carbonate saturation [*Hoegh-Guldberg et al.*, 2007; *De'ath et al.*, 2009]. We suggest that as Cenozoic pCO_2 dipped below the 480 ppm threshold, long-term ocean de-acidification provided a more suitable environment for coral reef proliferation. This pCO_2 threshold was reached after the seawater Mg/Ca threshold, in the late Oligocene to early Miocene [*Pagani et al.*, 2005]. Therefore, while increasing seawater Mg/Ca in the early Cenozoic "preconditioned" the oceans to be favorable for aragonite-precipitating organisms, the decreased pCO_2 and increased seawater saturation state caused by ocean de-acidification may have ultimately promoted the success of the coral reef ecosystem.

4. Conclusions

[34] Here we verify that the relationship between gastropod Sr/Ca and temperature is preserved in the fossil record. We use intrashell seasonal Sr/Ca and $\delta^{18}O$ cycles to produce new temperature calibrations based on our fossil shells. These have slopes of 0.15 ± 0.10 (1 s.d.) mmol mol^{-1} per °C for *Conus* and 0.10 ± 0.05 (1 s.d.) mmol mol^{-1} per °C for turritellid gastropods. Using the new calibrations and our Cenozoic record of gastropod Sr/Ca we present a new seawater Sr/Ca reconstruction from 42 Ma to present. By incorporating realistic uncertainties in the temperature calibrations of now extinct species we show that the gastropod record is higher but within error of published seawater Sr/Ca records derived using benthic foraminifera and fish teeth. Further investigation of the controls on gastropod shell Sr/Ca are needed to narrow the range of calculated seawater Sr/Ca. The reconstructed Paleogene seawater Sr/Ca values based on all three biogenic proxies are markedly higher than those derived from calcite veins precipitated in submarine basalts. We use a simple Sr flux model to suggest that the uncertainties and assumptions in using calcite veins to reconstruct Sr/Ca_{sw} need to be revisited. Finally, we estimate global average DSr_{SHELF} values for the past 33 Ma and suggest that the Neogene increase in the proportion of aragonite to calcite deposition is

likely linked to ocean de-acidification on these geological timescales.

Acknowledgments

[35] We thank T. Kobashi, who helped launch this study through his isotopic study of paleoclimates and B. N. Opdyke and J. Caves for helpful discussions. Samples were provided by T. Kobashi, D. Dockery and the Mississippi Office of Environmental Quality. We thank Anthony Coates, Helena Fortunato, Jeremy Jackson, Jill Leonard Pingel and Felix Rodriguez for helping collect sample material and *Recursos Minerales* for granting permits for Panama specimen collection. We acknowledge support from the NSF (EAR-0126311 to ELG, EAR-0126173 to YR and CHL, and EAR03–45471 to AO), the National Geographic Society to AO, the U.S.-UK Fulbright Fellowship to SMS, the Michel T. Halbouty Chair in Geology (TAMU), and the National System of Investigators (SNI) of the National Research of the National Secretariat for Science, Technology and Innovation of Panama (SENACYT) to AO.

References

Allmon, W. D. (1993), Age, environment and mode of deposition of the densely fossiliferous Pinecrest Sand (Pliocene of Florida): Implications for the role of biological productivity in shell bed formation, *Palaios*, *8*, 183–201, doi:10.2307/3515171.

Alt, J. C. (2003), Hydrothermal fluxes at mid-ocean ridges and on ridge flanks, *C. R. Geosci.*, *335*(10–11), 853–864, doi:10.1016/j.crte.2003.02.001.

Arvidson, R. S., F. T. Mackenzie, and M. Guidry (2006), MAGic: A Phanerozoic model for the geochemical cycling of major rock-forming components, *Am. J. Sci.*, *306*(3), 135–190, doi:10.2475/ajs.306.3.135.

Averyt, K. B., and A. Paytan (2002), Cenozoic seawater Sr/Ca ratio curve from marine barite: A preliminary investigation, *Eos Trans. AGU*, *83*(4), Ocean Sci. Meet. Suppl., Abstract OS32A-119.

Averyt, K. B., and A. Paytan (2003), Empirical partition coefficients for Sr and Ca in marine barite: Implications for reconstructing seawater Sr and Ca concentrations, *Geochem. Geophys. Geosyst.*, *4*(5), 1043, doi:10.1029/2002GC000426.

Balter, V. (2004), Allometric constraints on Sr/Ca and Ba/Ca partitioning in terrestrial mammalian trophic chains, *Oecologia*, *139*(1), 83–88, doi:10.1007/s00442-003-1476-0.

Balter, V., and C. Lécuyer (2010), Determination of Sr and Ba partition coefficients between apatite from fish (*Sparus aurata*) and seawater: The influence of temperature, *Geochim. Cosmochim. Acta*, *74*(12), 3449–3458, doi:10.1016/j.gca.2010.03.015.

Balter, V., C. Lécuyer, and J.-A. Barrat (2011), Reconstructing seawater Sr/Ca during the last 70 My using fossil fish tooth enamel, *Palaeogeogr. Palaeoclimatol. Palaeoecol.*, *310*(1–2), 133–138, doi:10.1016/j.palaeo.2011.02.024.

Berggren, W. A., D. V. Kent, C. C. Swisher III, and M.-P. Aubry (1995), A revised Cenozoic geochronology and chronostratigraphy, in *Geochronology, Time Scales, and Stratigraphic Correlation*, pp. 129–212, Soc. for Sediment. Geol., Tulsa, Okla.

Berner, E. K., and R. A. Berner (1996), *Global Environment: Water, Air and Geochemical Cycles*, Princeton Univ. Press, Princeton, N. J.

Berner, R. A. (1994), GEOCARB-II–A revised model of atmospheric CO_2 over Phanerozoic time, *Am. J. Sci.*, *294*(1), 56–91, doi:10.2475/ajs.294.1.56.

Berner, R. A., A. C. Lasaga, and R. M. Garrels (1983), The carbonate-silicate geochemical cycle and its effects on atmospheric carbon-dioxide over the past 100 million years, *Am. J. Sci.*, *283*(7), 641–683, doi:10.2475/ajs.283.7.641.

Bluth, G. J. S., and L. R. Kump (1991), Phanerozoic paleogeology, *Am. J. Sci.*, *291*(3), 284–308, doi:10.2475/ajs.291.3.284.

Broecker, W. S., and T. H. Peng (1982), *Tracers in the Sea*, Eldigio, New York.

Broecker, W., and J. Yu (2011), What do we know about the evolution of Mg to Ca ratios in seawater?, *Paleoceanography*, *26*, PA3203, doi:10.1029/2011PA002120.

Bryant, J. D., B. J. Macfadden, and P. A. Mueller (1992), Improved chronological resolution of the Hawthorn and the Alum Bluff Groups in northern Florida–Implications for Miocene chronostratigraphy, *Geol. Soc. Am. Bull.*, *104*, 208–218, doi:10.1130/0016-7606(1992)104<0208:ICROTH>2.3.CO;2.

Buchardt, B., and P. Fritz (1978), Strontium uptake in shell aragonite from freshwater gastropod *Limnae stagnalis*, *Science*, *199*(4326), 291–292, doi:10.1126/science.199.4326.291.

Carpenter, S. J., and K. C. Lohmann (1992), Sr/Mg ratios of modern marine calcite: Empirical indicators of ocean chemistry and precipitation rate, *Geochim. Cosmochim. Acta*, *56*(5), 1837–1849, doi:10.1016/0016-7037(92)90314-9.

Coates, A. G. (1999), Lithostratigraphy of the Neogene strata of the Caribbean coast from Limon, Costa Rica, to Colon, *Bull. Am. Paleontol.*, *357*, 17–40.

Coates, A. G., J. B. C. Jackson, L. S. Collins, T. M. Cronin, H. J. Dowsett, L. M. Bybell, P. Jung, and J. A. Obando (1992), Closuer of the isthmus of Panama–The near-shore marine record of Costa Rica and western Panama, *Geol. Soc. Am. Bull.*, *104*(7), 814–828, doi:10.1130/0016-7606(1992)104<0814:COTIOP>2.3.CO;2.

Coates, A. G., D. F. McNeill, M. P. Aubry, W. A. Berggren, and L. S. Collins (2005), An introduction to the geology of the Bocas del Toro archipelago, Panama, *Caribb. J. Sci.*, *41*(3), 374–391.

Coggon, R. M., D. A. H. Teagle, C. E. Smith-Duque, J. C. Alt, and M. J. Cooper (2010), Reconstructing past seawater Mg/Ca and Sr/Ca from mid-ocean ridge flank calcium carbonate veins, *Science*, *327*(5969), 1114–1117, doi:10.1126/science.1182252.

Coggon, R. M., D. A. H. Teagle, and T. D. Jones (2011), Comment on "What do we know about the evolution of Mg to Ca ratios in seawater?" by Wally Broecker and Jimin Yu, *Paleoceanography*, *26*, PA3224, doi:10.1029/2011PA002186.

Conrad, C. P., and C. Lithgow-Bertelloni (2007), Faster seafloor spreading and lithosphere production during the mid-Cenozoic, *Geology*, *35*(1), 29–32, doi:10.1130/G22759A.1.

Cotton, M. A. (1999), Neogene planktonic foraminiferal biochronology of the southern Central American isthmus, *Bull. Am. Paleontol.*, *357*, 1–80.

De'ath, G., J. M. Lough, and K. E. Fabricius (2009), Declining coral calcification on the Great Barrier Reef, *Science*, *323*(5910), 116–119, doi:10.1126/science.1165283.

Delaney, M. L., and E. A. Boyle (1986), Lithium in foraminiferal shells: Implications for high-temperature hydrothermal circulation fluxes and oceanic crustal generation rates, *Earth*

Planet. Sci. Lett., *80*(1–2), 91–105, doi:10.1016/0012-821X(86)90022-1.

De La Rocha, C. L., and D. J. DePaolo (2000), Isotopic evidence for variations in the marine calcium cycle over the Cenozoic, *Science*, *289*(5482), 1176–1178, doi:10.1126/science.289.5482.1176.

DePaolo, D. J. (2004), Calcium isotopic variations produced by biological, kinetic, radiogenic, and nucleosynthetic processes, *Rev. Mineral. Geochem.*, *55*, 255–288, doi:10.2138/gsrmg.55.1.255.

de Villiers, S. (1999), Seawater strontium and Sr/Ca variability in the Atlantic and Pacific oceans, *Earth Planet. Sci. Lett.*, *171*(4), 623–634, doi:10.1016/S0012-821X(99)00174-0.

Dickson, J. A. D. (2002), Fossil echinoderms as monitor of the Mg/Ca ratio of phanerozoic oceans, *Science*, *298*(5596), 1222–1224, doi:10.1126/science.1075882.

Dissard, D., G. Nehrke, G. J. Reichart, and J. Bijma (2010), Impact of seawater pCO_2 on calcification and Mg/Ca and Sr/Ca ratios in benthic foraminifera calcite: Results from culturing experiments with *Ammonia tepida*, *Biogeosciences*, *7*(1), 81–93, doi:10.5194/bg-7-81-2010.

Dockery, D. T., III (1980), The invertebrate macropaleontology of the Clark County, Mississippi area, *Miss. Bur. Geol. Bull.*, *122*, 1–387.

Dockery, D. T., III (1996), Toward a revision of the generalized stratigraphic column of Mississippi, *Miss. Geol.*, *17*, 1–7.

Dueñas-Bohórquez, A., R. E. da Rocha, A. Kuroyanagi, J. Bijma, and G.-J. Reichart (2009), Effect of salinity and seawater calcite saturation state on Mg and Sr incorporation in cultured planktonic foraminifera, *Mar. Micropaleontol.*, *73*(3–4), 178–189, doi:10.1016/j.marmicro.2009.09.002.

Dueñas-Bohórquez, A., M. Raitzsch, L. J. de Nooijer, and G.-J. Reichart (2011), Independent impacts of calcium and carbonate ion concentration on Mg and Sr incorporation in cultured benthic foraminifera, *Mar. Micropaleontol.*, *81*(3–4), 122–130, doi:10.1016/j.marmicro.2011.08.002.

Edmond, J. M., C. Measures, R. E. McDuff, L. H. Chan, R. Collier, B. Grant, L. I. Gordon, and J. B. Corliss (1979), Ridge crest hydrothermal activitiy and the balances of the major and minor elements in the ocean-Galapagos data, *Earth Planet. Sci. Lett.*, *46*(1), 1–18, doi:10.1016/0012-821X(79)90061-X.

Elderfield, H., and A. Schultz (1996), Mid-ocean ridge hydrothermal fluxes and the chemical composition of the ocean, *Annu. Rev. Earth Planet. Sci.*, *24*, 191–224, doi:10.1146/annurev.earth.24.1.191.

Elderfield, H., C. J. Bertram, and J. Erez (1996), Biomineralization model for the incorporation of trace elements into foraminiferal calcium carbonate, *Earth Planet. Sci. Lett.*, *142*(3–4), 409–423, doi:10.1016/0012-821X(96)00105-7.

Elderfield, H., M. Vautravers, and M. Cooper (2002), The relationship between shell size and Mg/Ca, Sr/Ca, $\delta^{18}O$, and $\delta^{13}C$ of species of planktonic foraminifera, *Geochem. Geophys. Geosyst.*, *3*(8), 1052, doi:10.1029/2001GC000194.

Gaillardet, J., B. Dupre, P. Louvat, and C. J. Allegre (1999), Global silicate weathering and CO_2 consumption rates deduced from the chemistry of large rivers, *Chem. Geol.*, *159*(1–4), 3–30, doi:10.1016/S0009-2541(99)00031-5.

Gentry, D. K., S. Sosdian, E. L. Grossman, Y. Rosenthal, D. Hicks, and C. H. Lear (2008), Stable isotope and Sr/Ca profiles from the marine gastropod Conus ermineus: Testing a multiproxy approach for inferring paleotemperature and paleosalinity, *Palaios*, *23*(4), 195–209, doi:10.2110/palo.2006.p06-112r.

Gibbs, M. T., G. J. S. Bluth, P. J. Fawcett, and L. R. Kump (1999), Global chemical erosion over the last 250 my: Variations due to changes in paleogeography, paleoclimate, and paleogeology, *Am. J. Sci.*, *299*(7–9), 611–651, doi:10.2475/ajs.299.7-9.611.

Graham, D. W., M. L. Bender, D. F. Williams, and L. D. Keigwin (1982), Strontium-calcium ratios in Cenozoic planktonic foraminifera, *Geochim. Cosmochim. Acta*, *46*(7), 1281–1292, doi:10.1016/0016-7037(82)90012-6.

Grossman, E. L., and T. L. Ku (1986), Oxygen and carbon isotope fractionation in biogenic aragonite: Temperature effects, *Chem. Geol.*, *59*(1), 59–74, doi:10.1016/0168-9622(86)90057-6.

Hardie, L. A. (1996), Secular variation in seawater chemistry: An explanation for the coupled secular variation in the mineralogies of marine limestones and potash evaporites over the past 600 my, *Geology*, *24*(3), 279–283, doi:10.1130/0091-7613(1996)024<0279:SVISCA>2.3.CO;2.

Hoegh-Guldberg, O., et al. (2007), Coral reefs under rapid climate change and ocean acidification, *Science*, *318*(5857), 1737–1742, doi:10.1126/science.1152509.

Holmden, C., R. A. Creaser, and K. Muehlenbachs (1997), Paleosalinities in ancient brackish water systems determined using $^{87}Sr/^{88}Sr$ ratios in carbonate fossils: A case study from the Western Canada Sedimentary Basin, *Geochim. Cosmochim. Acta*, *46*, 1281–1292.

Horita, J., H. Zimmermann, and H. D. Holland (2002), Chemical evolution of seawater during the Phanerozoic: Implications from the record of marine evaporites, *Geochim. Cosmochim. Acta*, *66*(21), 3733–3756, doi:10.1016/S0016-7037(01)00884-5.

Ivany, L. C., B. H. Wilkinson, K. C. Lohmann, E. R. Johnson, B. J. McElroy, and G. J. Cohen (2004), Intra-annual isotopic variation in Venericardia bivalves: Implications for early Eocene temperature, seasonality, and salinity on the US Gulf Coast, *J. Sediment. Res.*, *74*(1), 7–19, doi:10.1306/052803740007.

Katz, A., A. Starinsk, E. Sass, and H. D. Holland (1972), Strontium behavior in aragonite-calcite transformation: Experimental study at 40°C, *Geochim. Cosmochim. Acta*, *36*(4), 481, doi:10.1016/0016-7037(72)90037-3.

Kiessling, W. (2009), Geologic and biologic controls on the evolution of reefs, *Ann. Rev. Ecol. Evol. Syst.*, *40*, 173–192.

Kinsman, D. J. J., and H. D. Holland (1969), Co-precipitation of cations with $CACO_3$. 4. co-precipitation of SR^{2+} with aragonite between 16° and 96°C, *Geochim. Cosmochim. Acta*, *33*(1), 1, doi:10.1016/0016-7037(69)90089-1.

Kobashi, T., E. L. Grossman, T. E. Yancey, and D. T. Dockery (2001), Reevaluation of conflicting Eocene tropical temperature estimates: Molluskan oxygen isotope evidence for warm low latitudes, *Geology*, *29*(11), 983–986, doi:10.1130/0091-7613(2001)029<0983:ROCETT>2.0.CO;2.

Land, L. S. (1967), Diagenesis of skeletal carbonates, *J. Sediment. Petrol.*, *37*, 914–930.

Lear, C. H., and Y. Rosenthal (2006), Benthic foraminiferal Li/Ca: Insights into Cenozoic seawater carbonate saturation state, *Geology*, *34*(11), 985–988, doi:10.1130/G22792A.1.

Lear, C. H., H. Elderfield, and P. A. Wilson (2000), Cenozoic deep-sea temperatures and global ice volumes from Mg/Ca in benthic foraminiferal calcite, *Science*, *287*(5451), 269–272, doi:10.1126/science.287.5451.269.

Lear, C. H., Y. Rosenthal, and N. Slowey (2002), Benthic foraminiferal Mg/Ca- paleothermometry: A revised core-top

calibration, *Geochim. Cosmochim. Acta*, *66*(19), 3375–3387, doi:10.1016/S0016-7037(02)00941-9.

Lear, C. H., H. Elderfield, and P. A. Wilson (2003), A Cenozoic seawater Sr/Ca record from benthic foraminiferal calcite and its application in determining global weathering fluxes, *Earth Planet. Sci. Lett.*, *208*(1–2), 69–84, doi:10.1016/S0012-821X(02)01156-1.

Leon-Rodriguez, L. (2007), Benthic foraminiferal record of the Pleistocene uplift of the sedimentary deposits of the Burica Peninsula (Costa Rica-Panama) as a result of Cocos Ridge subduction beneath the Central American Arc, MS thesis, 97 pp., Fla. Intl. Univ., Miami.

Lorens, R. B., and M. L. Bender (1980), The impact of solution chemistry on *Mytilus edulis* calcite and aragonite, *Geochim. Cosmochim. Acta*, *44*(9), 1265–1278, doi:10.1016/0016-7037(80)90087-3.

Lowenstein, T. K., M. N. Timofeeff, S. T. Brennan, L. A. Hardie, and R. V. Demicco (2001), Oscillations in Phanerozoic seawater chemistry: Evidence from fluid inclusions, *Science*, *294*(5544), 1086–1088, doi:10.1126/science.1064280.

Mancini, E. A., and B. H. Tew (1991), Relationships of Paleogene stage and planktonic foraminiferal zone boundaries to lithostratigraphic and allostratigraphic contacts in the eastern Gulf Coastal plain, *J. Foraminiferal Res.*, *21*, 48–66, doi:10.2113/gsjfr.21.1.48.

Meybeck, M., and A. Ragu (1996), River discharges to the oceans. An assessment of suspended solids, major ions, and nutrients, in *Environment Information and Assessment Report*, pp. 1–250, U. N. Environ. Programme, Nairobi, Africa.

Mucci, A., and J. W. Morse (1983), The incorporation of Mg^{2+} and Sr^{2+} into calcite overgrowths- Influences of growth rate and solution composition, *Geochim. Cosmochim. Acta*, *47*(2), 217–233, doi:10.1016/0016-7037(83)90135-7.

Müller, R. D., M. Sdrolias, C. Gaina, B. Steinberger, and C. Heine (2008), Long-term sea-level fluctuations driven by ocean basin dynamics, *Science*, *319*(5868), 1357–1362, doi:10.1126/science.1151540.

Nakamori, T. (2001), Global carbonate accumulation rates from Cretaceous to present and their implications for the carbon cycle model, *Isl. Arc*, *10*, 1–8, doi:10.1046/j.1440-1738.2001.00276.x.

Opdyke, B. N., and B. H. Wilkinson (1988), Surface area control of shallow cratonic to deep marine carbonate accumulation, *Paleoceanography*, *3*(6), 685–703, doi:10.1029/PA003i006p00685.

Opdyke, B. N., P. A. Wilson, and P. Enos (1995), Geochemistry diagenesis, and petrology of an upper Cretaceous rudist reef from site 877, Wodejebato Guyot, *Proc. Ocean Drill. Program Sci. Results*, *144*, 439–446, doi:10.2973/odp.proc.sr.144.053.1995.

Pagani, M., J. C. Zachos, K. H. Freeman, B. Tipple, and S. Bohaty (2005), Marked decline in atmospheric carbon dioxide concentrations during the Paleogene, *Science*, *309*(5734), 600–603, doi:10.1126/science.1110063.

Palmer, M. R., and J. M. Edmond (1989), The strontium isotope budget of the modern ocean, *Earth Planet. Sci. Lett.*, *92*, 11–26, doi:10.1016/0012-821X(89)90017-4.

Purton, L. M. A., G. A. Shields, M. D. Brasier, and G. W. Grime (1999), Metabolism controls Sr/Ca ratios in fossil aragonitic mollusks, *Geology*, *27*(12), 1083–1086.

Raitzsch, M., A. Dueñas-Bohórquez, G. J. Reichart, L. J. de Nooijer, and T. Bickert (2010), Incorporation of Mg and Sr in calcite of cultured benthic foraminifera: Impact of calcium concentration and associated calcite saturation state, *Biogeosciences*, *7*(3), 869–881.

Ravizza, G. E., and J. C. Zachos (2003), Records of Cenozoic ocean chemistry, in *Treatise on Geochemistry*, vol. 6, *The Oceans and Marine Chemistry*, edited by H. Elderfield, pp. 551–582, Elsevier, Amsterdam.

Rosenthal, Y., E. A. Boyle, and N. Slowey (1997), Temperature control on the incorporation of magnesium, strontium, fluorine, and cadmium into benthic foraminiferal shells from Little Bahama Bank: Prospects for thermocline paleoceanography, *Geochim. Cosmochim. Acta*, *61*(17), 3633–3643, doi:10.1016/S0016-7037(97)00181-6.

Schlanger, S. O. (1988), Strontium storage and release during deposition and diagenesis of marine carbonates related to sea-level variations, in *Physical and Chemical Weathering in Geochemical Cycles*, edited by A. Lerman and M. Meybeck, pp. 323–339, Kluwer, Dordrecht, Netherlands, doi:10.1007/978-94-009-3071-1_15.

Schmidt, M. W., H. J. Spero, and D. W. Lea (2004), Links between salinity variation in the Caribbean and North Atlantic thermohaline circulation, *Nature*, *428*(6979), 160–163, doi:10.1038/nature02346.

Scott, T. M. (2011), Geology of the Florida platform pre-Mesozoic to Recent, in *Gulf of Mexico Origin, Waters, and Biota*, vol. 3, *Geology*, edited by N. A. Buster and C. W. Holmes, pp. 17–32, Texas A&M Univ. Press, College Station, Tex.

Sosdian, S., D. K. Gentry, C. H. Lear, E. L. Grossman, D. Hicks, and Y. Rosenthal (2006), Strontium to calcium ratios in the marine gastropod *Conus ermineus*: Growth rate effects and temperature calibration, *Geochem. Geophys. Geosyst.*, *7*, Q11023, doi:10.1029/2005GC001233.

Stanley, S. M., and L. A. Hardie (1998), Secular oscillations in the carbonate mineralogy of reef-building and sediment-producing organisms driven by tectonically forced shifts in seawater chemistry, *Palaeogeogr. Palaeoclimatol. Palaeoecol.*, *144*(1–2), 3–19, doi:10.1016/S0031-0182(98)00109-6.

Steuber, T., and A. Veizer (2002), Phanerozoic record of plate tectonic control of seawater chemistry and carbonate sedimentation, *Geology*, *30*(12), 1123–1126, doi:10.1130/0091-7613(2002)030<1123:PROPTC>2.0.CO;2.

Stoll, H. M., and D. P. Schrag (1998), Effects of Quaternary sea level cycles on strontium in seawater, *Geochim. Cosmochim. Acta*, *62*(7), 1107–1118, doi:10.1016/S0016-7037(98)00042-8.

Stoll, H. M., and D. P. Schrag (2000), Coccolith Sr/Ca as a new indicator of coccolithophorid calcification and growth rate, *Geochem. Geophys. Geosyst.*, *1*(5), 1006, doi:10.1029/1999GC000015.

Tao, K. (2012), *Neogene Low-Latitude Seasonal Environmental Variations: Stable Isotopic and Trace Elemental Records in Mollusks From the Florida Platform and the Central American Isthmus*, Texas A&M Univ., College Station, Tex.

Tao, K., and E. L. Grossman (2010), Origin of high productivity in the Pliocene of the Florida platform evidence from stable isotopes and trace elements, *Palaios*, *25*(12), 796–806, doi:10.2110/palo.2010.p10-058r.

Tripati, A. K., W. D. Allmon, and D. E. Sampson (2009), Possible evidence for a large decrease in seawater strontium/calcium ratios and strontium concentrations during the Cenozoic, *Earth Planet. Sci. Lett.*, *282*(1–4), 122–130, doi:10.1016/j.epsl.2009.03.020.

Turekian, K. K. (1964), The marine geochemistry of strontium, *Geochim. Cosmochim. Acta*, *28*, 1479–1496, doi:10.1016/0016-7037(64)90163-2.

Vance, D., D. A. H. Teagle, and G. L. Foster (2009), Variable Quaternary chemical weathering fluxes and imbalances in

marine geochemical budgets, *Nature*, *458*, 493–496, doi:10.1038/nature07828.

Wilkinson, B. H., and T. J. Algeo (1989), Sedimentary carbonate record of calcium magnesium cycling, *Am. J. Sci.*, *289*(10), 1158–1194, doi:10.2475/ajs.289.10.1158.

Williams, M., A. M. Haywood, E. M. Harper, A. L. A. Johnson, T. Knowles, M. J. Leng, D. J. Lunt, B. Okamura, P. D. Taylor, and J. Zalasiewicz (2009), Pliocene climate and seasonality in North Atlantic shelf seas, *Philos. Trans. R. Soc. A*, *367*(1886), 85–108.

Zachos, J. C., L. D. Stott, and K. C. Lohmann (1994), Evolution of early Cenozoic marine temperatures, *Paleoceanography*, *9*(2), 353–387, doi:10.1029/93PA03266.